A Survey on Sparse Autoencoders:
Interpreting the Internal Mechanisms of Large Language Models

Dong Shu[1,†], Xuansheng Wu[2,†], Haiyan Zhao[3,†], Daking Rai[4],
Ziyu Yao[4], Ninghao Liu[2], Mengnan Du[3]
[1]Northwestern University [2]University of Georgia
[3]New Jersey Institute of Technology [4]George Mason University
dongshu2024@u.northwestern.edu, {xw54582,ninghao.liu}@uga.edu,
{hz54,mengnan.du}@njit.edu, {drai2,ziyuyao}@gmu.edu

Abstract

Large Language Models (LLMs) have transformed natural language processing, yet their internal mechanisms remain largely opaque. Recently, mechanistic interpretability has attracted significant attention from the research community as a means to understand the inner workings of LLMs. Among various mechanistic interpretability approaches, Sparse Autoencoders (SAEs) have emerged as a promising method due to their ability to disentangle the complex, superimposed features within LLMs into more interpretable components. This paper presents a comprehensive survey of SAEs for interpreting and understanding the internal workings of LLMs. Our major contributions include: (1) exploring the technical framework of SAEs, covering basic architecture, design improvements, and effective training strategies; (2) examining different approaches to explaining SAE features, categorized into input-based and output-based explanation methods; (3) discussing evaluation methods for assessing SAE performance, covering both structural and functional metrics; and (4) investigating real-world applications of SAEs in understanding and manipulating LLM behaviors.

1 Introduction

Large Language Models (LLMs), such as GPT-4 (OpenAI et al., 2024), Claude-3.5 (Anthropic, 2024), DeepSeek-R1 (DeepSeek-AI et al., 2025), and Grok-3 (xAI, 2025), have emerged as powerful tools in natural language processing, demonstrating remarkable capabilities in tasks ranging from text generation to complex reasoning. However, their increasing size and complexity have created significant challenges in understanding their internal representations and decision-making processes. This "black box" nature of LLMs has sparked a growing interest in mechanistic interpretability (Bereska and Gavves, 2024a; Zhao et al., 2024a; Rai et al.,

2024; Zhao et al., 2024b), a field that aims to break down LLMs into understandable components and systematically analyze how these components interact to understand their behaviors.

Among the various approaches to interpreting LLMs, Sparse Autoencoders (SAEs) (Cunningham et al., 2023; Bricken et al., 2023; Gao et al., 2025; Rajamanoharan et al., 2024b; Galichin et al., 2025) have emerged as a particularly promising direction for addressing a fundamental challenge in LLM interpretability: *polysemanticity*. Many neurons in LLMs are polysemantic, responding to seemingly unrelated concepts or features simultaneously. This is a phenomenon likely resulting from superposition (Elhage et al., 2022), where LLMs represent more independent features than they have neurons by encoding each feature as a linear combination of neurons. SAEs address this issue by learning an overcomplete, sparse representation of neural activations, effectively disentangling these superimposed features into more interpretable units. By training a sparse autoencoder to reconstruct the activations of a target network layer while enforcing sparsity constraints, SAEs can extract a larger set of *monosemantic* features that offer clearer insights into what information the LLM is processing. This approach has shown promise in transforming the often-inscrutable activations of LLMs into more human-understandable representations, potentially creating a more effective vocabulary for mechanistic analysis of these complex systems.

1.1 Contribution and Uniqueness

Our Contributions. In this paper, we provide a comprehensive overview of SAE for LLM interpretability, with major contributions listed as following: (1) We explore the technical framework of SAEs, including their basic architecture, various design improvements, and effective training strategies (Section 2). (2) We examine different approaches to analyzing and explaining SAE features,
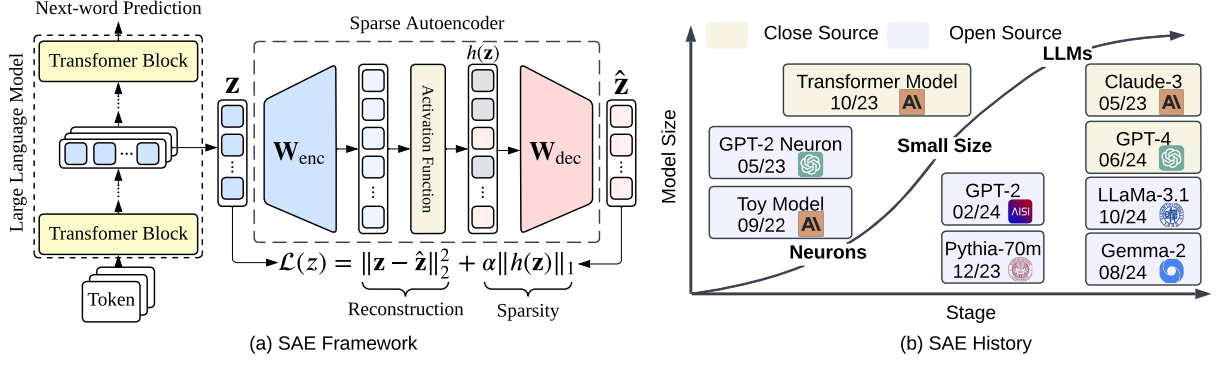
Figure 1: (a) This figure illustrates the fundamental framework of a Sparse Autoencoder (SAE). SAE is trained to take a model representation $\mathbf{z}$ as input and project it to an overcomplete sparse activation $h(\mathbf{z})$ by learning to reconstruct the original input $\hat{\mathbf{z}}$. The SAE typically comprises an encoder, a decoder, and a loss function for training. (b) The development of the SAE progresses through multiple stages. Note that we only list some representative SAE models in this timeline rather than providing an exhaustive compilation.

categorized broadly into input-based and output-based explanation methods (Section 3). (3) We discuss evaluation methodologies for assessing SAE performance, covering both structural metrics and functional metrics (Section 4). (4) We discuss real-world applications of SAEs in understanding and manipulating LLMs (Section 5). (5) Additionally, in the appendix, we also introduce key motivations for SAE, discuss connection of SAEs to the broader field of mechanistic interpretability, provide experimental evaluations, and highlight current research challenges and promising future directions.

Differences with Existing Surveys. Several existing surveys take a broad perspective on LLM interpretability. For instance, some surveys provide comprehensive overviews of general explainability methods for LLMs (Ferrando et al., 2024; Zhao et al., 2024a), while others focus specifically on mechanistic interpretability as a whole (Rai et al., 2024; Bereska and Gavves, 2024b). In contrast, our work uniquely focuses exclusively on SAEs as a specific and promising approach within the mechanistic interpretability landscape. By narrowing our scope to SAEs, we are able to provide a much more comprehensive and detailed analysis of their principles, architectures, training methodologies, evaluation techniques, and practical applications.

2 Technical Framework of SAEs

2.1 Basic SAE Framework

SAE is a neural network that learns an overcomplete dictionary for representation reconstruction. As shown in Figure 1a, the input of SAE is the representation of a token from LLMs, which is mapped onto a sparse vector of dictionary activations.

Input. Given a LLM denoted as f with a total of L transformer layers, we consider an input sequence $x = (x_0, \ldots, x_N)$ with N tokens, where each $x_n \in x$ represents a token in the sequence. As the sequence x is processed by the LLM, each token x_n produces representations at different layers. For a specific layer l, we denote the hidden representation corresponding to token x_n as $\mathbf{z}_n^{(l)}$, where $\mathbf{z}_n^{(l)} \in \mathbb{R}^d$ indicates the embedding vector of dimension d. Each representation $\mathbf{z}_n^{(l)}$ serves as input to SAEs. In the following, we may omit the superscript $^{(l)}$ of layers to simplify the notation.

After extracting the representation $\mathbf{z}_n^{(l)}$, the SAE takes it as input, decomposes it into a sparse representation, and then reconstructs it. The SAE framework is typically composed of three key components: the *encoder*, which maps the input representation to a higher-dimensional sparse activation; the *decoder*, which reconstructs the original representation from this sparse activation; and the *loss function*, which ensures accurate reconstruction while enforcing sparsity constraints.

Encoding Step. Given an input representation $\mathbf{z} \in \mathbb{R}^d$, the encoder applies a linear transformation using a weight matrix $\mathbf{W}_{\text{enc}} \in \mathbb{R}^{d \times m}$ and a bias term $\mathbf{b}_{\text{enc}} \in \mathbb{R}^m$, followed by an activation function σ to enforce sparsity. The encoding operation is defined as:

$$h(\mathbf{z}) = \sigma \left(\mathbf{z} \cdot \mathbf{W}_{\text{enc}} + \mathbf{b}_{\text{enc}} \right), \qquad (1)$$

where $h(\mathbf{z}) \in \mathbb{R}^m$ represents the sparse activation vector, which helps disentangle superposition features. The σ activation function could take differ-

Table 1: Taxonomy of SAE Frameworks: An Overview of Basic and Variant Architectures.

Category	Examples	Activation	Citations
Basic SAE Framework (§2.1)	l_2-norm SAE	ReLU	Ferrando et al. (2024)
Improve Architecture (§C.1)	Gated SAE	Jump ReLU	Rajamanoharan et al. (2024a)
	TopK SAE	TopK	Gao et al. (2025)
	Batch TopK SAE	Batch TopK	Bussmann et al. (2024)
	ProLU SAE	ProLU	Taggart (2024)
	JumpReLU SAE	Jump ReLU	Rajamanoharan et al. (2024b)
	Switch SAE	TopK	Mudide et al. (2024)
Improve Training Strategy (§C.2)	Layer Group SAE	Jump ReLU	Ghilardi et al. (2024)
	Feature Choice SAE	TopK	Ayonrinde (2024)
	Mutual Choice SAE	TopK	Ayonrinde (2024)
	Feature Aligned SAE	TopK	Marks et al. (2024)
	End-to-end SAE	ReLU	Braun et al. (2025)
	Formal Languages SAE	ReLU	Menon et al. (2024)
	Specialized SAE	ReLU	Muhamed et al. (2024)

ent formats (see Table 1). For example, σ could be ReLU $(x) = \max(0, x)$, ensures that only non-negative values pass through, encouraging sparsity by setting negative values to zero.

Since the SAE constructs an overcomplete dictionary to facilitate sparse activation, the number of learned dictionary elements m is chosen to be larger than the input dimension d (i.e., $m \gg d$). This overcompleteness allows the encoder to learn a richer and more expressive representation of the input, making it possible to reconstruct the original data using only a sparse subset of dictionary elements. The output $h(\mathbf{z})$ from the encoder is then passed to the decoding stage, where it is mapped back to the original input space to reconstruct $\mathbf{z}$.

Decoding Step. After the encoding step, the next stage in the SAE framework is the decoding process, where the sparse activation vector $h(\mathbf{z})$ is mapped back to the original input space. This step ensures that the sparse features learned by the encoder contain sufficient information to accurately reconstruct the original representation. The decoding operation is defined as:

$$\hat{\mathbf{z}} = SAE(\mathbf{z}) = h(\mathbf{z}) \cdot \mathbf{W}_{\text{dec}} + \mathbf{b}_{\text{dec}}, \quad (2)$$

where $\mathbf{W}_{\text{dec}} \in \mathbb{R}^{m \times d}$ is the decoder weight matrix. $\mathbf{b}_{\text{dec}} \in \mathbb{R}^d$ is the decoder bias term. $\hat{\mathbf{z}} \in \mathbb{R}^d$ is the reconstructed output, which aims to approximate the original input $\mathbf{z}$.

The accuracy of the reconstruction and the interpretability of the learned representation depends heavily on the effectiveness and sparsity of the activation vector $h(\mathbf{z})$. Therefore, the SAE is trained

using a loss function that balances minimizing the reconstruction error and enforcing sparsity. This trade-off ensures that the learned dictionary elements provide a compact yet expressive representation of the input data.

Loss Function. The activation vector $h(\mathbf{z})$ is encouraged to be sparse, meaning that most of its values should be zero. Take the ReLU activation for example, while the activation function after the encoder enforces basic sparsity by setting negative values to zero, it does not necessarily eliminate small positive values, which can still contribute to a dense representation. Therefore, additional sparsity enforcement is required. This is achieved using a sparsity regularization term in the loss function, which further promotes a minimal number of active features. Beyond enforcing sparsity, the SAE must also ensure that the learned sparse activation retains sufficient information to accurately reconstruct the original input $\mathbf{z}$. The loss function for training the SAE consists of two key components: *reconstruction loss* and *sparsity regularization*:

$$\mathcal{L}(\mathbf{z}) = \|\mathbf{z} - \hat{\mathbf{z}}\|_2^2 + \alpha \|h(\mathbf{z})\|_1, \quad (3)$$

where reconstruction loss ensures that the SAE learns to reconstruct the input data accurately, meaning the features encoded in the sparse representation must also be present in the input activations. On the other hand, sparsity regularization enforces sparsity by penalizing nonzero values in $h(\mathbf{z})$, and α is a hyper-parameter to control the penalty level of the sparsity. Specifically, without the sparsity loss, SAEs could simply memorize the

training data, reconstructing the input without disentangling meaningful features. However, once the sparsity loss is introduced, the model is forced to activate only a small subset of neurons for reconstructing the input activation. This constraint encourages the SAE to focus on the most informative and critical features to reconstruct the input activation. A higher value of α enforces stronger sparsity by shrinking more values in $h(\mathbf{z})$ to zero, but this may lead to information loss and degraded reconstruction quality. A lower value of α prioritizes reconstruction accuracy but may result in less sparsity, reducing the interpretability of the learned features. Thus, selecting an optimal α is crucial for achieving a balance between interpretability and accurate data representation.

2.2 Different SAE Variants

As SAEs continue to emerge as a powerful tool for interpreting the internal representations of LLMs, researchers have increasingly focused on refining and extending their capabilities. Various SAE variants have been proposed to address the limitations of traditional SAEs, each introducing improvements from different perspectives. In this section, we categorize these advancements into two main groups: Improve Architectural, which modify the structure and design of the traditional SAE, and Improve Training Strategy, which retain the original architecture but introduce novel methods to enhance training efficiency, feature selection, and sparsity enforcement. A taxonomy of representative SAE frameworks is presented in Table 1. Due to page limitations, examples for each group are provided in Appendix C.1 (Improved Architectural) and Appendix C.2 (Improved Training Strategy). We also discuss challenges encountered during SAE training in Appendix C.3.

3 Explainability Analysis of SAEs

This section aims to interpret the learned feature vectors from a trained SAE with natural language. Specifically, given a pre-defined vocabulary set $\mathcal{V}$, the goal of the explainability analysis is to extract a subset of words $\mathcal{I}_m \subset \mathcal{V}$ to represent the meaning of $\mathbf{w}_m = \mathbf{W}_{\text{dec}}[m]$, for $m = 1, ..., M$. Humans can understand the meaning of $\mathbf{w}_m$ by reading their natural language explanations $\mathcal{I}_m$. There are two lines of work for this purpose, namely the *input-based* and *output-based* methods. Figure 2 visualizes generated explanations of using different methods to interpret a learned feature vector.

3.1 Input-based Explanations

MaxAct. The most straightforward way to collect natural language explanation is by selecting a set of texts whose hidden representation can *maximally activate* a certain feature vector we are interpreting (Bricken et al., 2023; Lee et al., 2023). Formally, given a large corpus $\mathcal{X}$ where each text span $x \in \mathcal{V}^N$ consists of N words, the MaxAct strategy finds K text spans that could maximally activate our interested learned feature vector $\mathbf{w}_m$:

$$\mathcal{I}_m = \underset{\mathcal{X}' \subset \mathcal{X}, |\mathcal{X}| = K}{\arg\max} \sum_{x \in \mathcal{X}'} f_{<l}(x) \cdot \mathbf{w}_m^\top, \quad (4)$$

where $f_{<l}(x)$ indicates generating the hidden representation of input text x at the l-th layer, and l is the layer our SAE is trained for. This strategy is reasonable for interpreting weight vectors of SAEs because of the sparse nature of SAEs, which indicates that a learned feature vector should only be activated by a certain pattern/concept. Therefore, summarizing the most activated text spans can give us a clue to understanding the semantic meaning encoded by the learned feature vector.

PruningMaxAct. While MaxAct collects text spans that maximally activate a feature vector, these spans often contain extraneous or redundant phrases that can obscure the underlying concept. Building on the Neuron-to-Graph approach (Foote et al., 2023), researchers (Gao et al., 2025) introduce a *pruning* operation to remove irrelevant tokens from each text span, thereby retaining only the minimal context necessary to preserve strong activation. Formally, let $p(\cdot)$ be a pruning strategy that maps text x to $p(x)$, and let $p^{-1}(\cdot)$ recover the original text from its pruned version. The final pruned spans are then gathered via:

$$\mathcal{I}_m = \underset{\mathcal{X}' \subset p(\mathcal{X}), |\mathcal{X}'| = K}{\arg\max} \sum_{x \in \mathcal{X}'} f_{<l}(x) \cdot \mathbf{w}_m^\top,$$
$$\text{s.t. } \forall x \in p(\mathcal{X}), \frac{f_{<l}(p^{-1}(x)) \cdot \mathbf{w}_m^\top}{f_{<l}(x) \cdot \mathbf{w}_m^\top} \geq 0.5, \quad (5)$$

where the condition enforces that the pruned text $p(x)$ retains at least half of the original activation. In practice, $p(\cdot)$ can be instantiated by removing selected tokens or replacing them with padding. According to Gao et al. (2025), this PruningMaxAct technique yields higher recall (i.e., finds more relevant examples) but lower precision compared to the original MaxAct strategy.
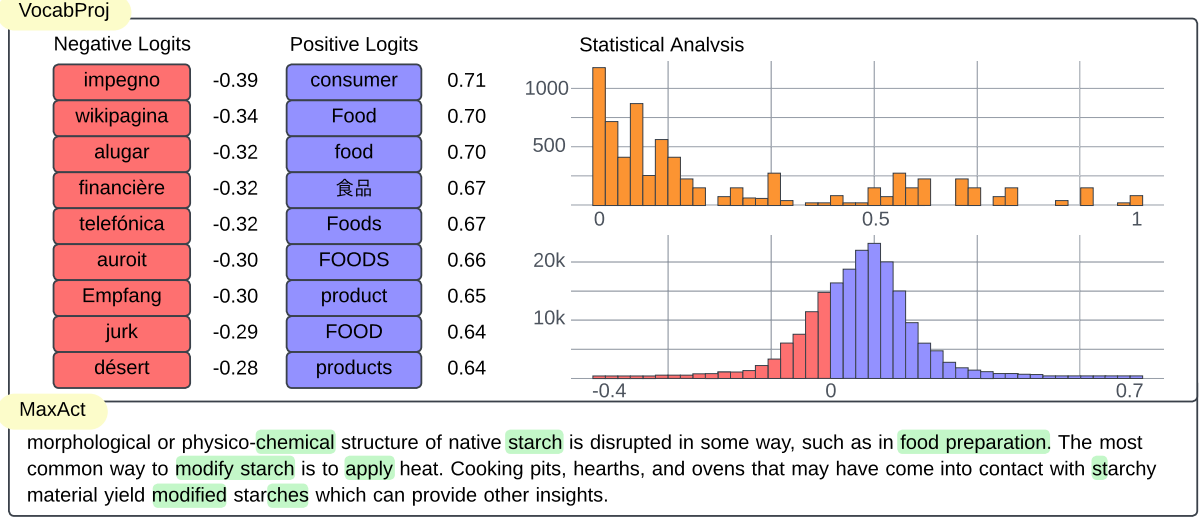
Figure 2: The figure illustrates the interpretation of a learned SAE feature using VocabProj and MaxAct. VocabProj lists words with the highest logits in "Positive Logits" column, and lowest logits in "Negative Logits" column. The upper histogram in Statistical Analysis shows the distribution of randomly sampled non-zero activations, with the y-axis representing the number of sampled activations and the x-axis indicating activation scores. The lower histogram depicts the logit density, where the y-axis represents the number of tokens and the x-axis corresponds to logit scores. MaxAct highlights tokens in an input text that strongly activate the learned feature. The figure references the Neuronpedia website (Lin, 2023).

3.2 Output-based Explanations

VocabProj. Output-based explanations project the learned feature vectors to the *output word embeddings* of words to compute the activations. Mathematically, $f_{\text{out}}(w) : \mathcal{V} \rightarrow \mathbb{R}^d$ denotes the output word embedding layer that returns the output embeddings of a word w, and we can collect the natural language explanations by:

$$\mathcal{I}_m = \underset{\mathcal{V}' \subset \mathcal{V}, |\mathcal{V}'|=K}{\arg\max} \sum_{w \in \mathcal{V}'} f_{\text{out}}(w) \cdot \mathbf{w}_m^\top. \quad (6)$$

This mapping process makes sense for decoder-only LLMs because the layers in such models share the same residual stream, enabling the representations in the intermediate layers to be linear correlated to the output word embeddings (Nostalgebraist, 2020). Recently, researchers (Wu et al., 2025b; Gur-Arieh et al., 2025) find that output-based explanations show a stronger promise in interpreting and controlling LLM behaviors (i.e., generated texts) compared to the input-based ones.

MutInfo. The VocabProj assumes that the output embeddings that maximally activate an interested feature vector can best describe the meaning of the learned feature. However, this assumption may fail for frequent words, whose embeddings often have large l_2 norm (Gao et al., 2019). To address this, Wu et al. (2025b) proposes extracting a vocabulary subset that maximizes mutual information with the learned feature. Formally, let $\mathcal{C}$ denote knowledge encoded by $\mathbf{w}_c$, the explanations are extracted by

$$\mathcal{I}_m = \underset{\mathcal{V}' \subset \mathcal{V}, |\mathcal{V}'|=M}{\arg\max} \text{MI}(\mathcal{V}'; \mathcal{C}) \propto \underset{\mathcal{V}' \subset \mathcal{V}, |\mathcal{V}'|=M}{\arg\min} \text{H}(\mathcal{C}|\mathcal{V}')$$
$$\propto \underset{\mathcal{V}' \subset \mathcal{V}, |\mathcal{V}'|=M}{\arg\max} \sum_{w \in \mathcal{V}'} p(w|\mathbf{w}_m) \log p(\mathbf{w}_m|w), \quad (7)$$

where $\text{MI}(\cdot; \cdot)$ indicates mutual information between two variables (Cover, 1999), $\text{H}(\cdot|\cdot)$ is the conditional entropy, and $U(\mathcal{C})$ includes all possible vectors that express the knowledge $\mathcal{C}$. Practically, the conditional probabilities can be estimated by:

$$p(w|\mathbf{w}_m) = \frac{\exp(f_{\text{out}}(w) \cdot \mathbf{w}_m^\top)}{\sum_{w' \in \mathcal{V}} \exp(f_{\text{out}}(w') \cdot \mathbf{w}_m^\top)},$$
$$p(\mathbf{w}_c|w) = \frac{\exp(f_{\text{out}}(w) \cdot \mathbf{w}_c^\top)}{\sum_{c' \in \mathcal{C}} \exp(f_{\text{out}}(w) \cdot \mathbf{W}_{c'}^\top)}. \quad (8)$$

Compared with VocabProj, that only considers $p(w|\mathbf{w}_m)$, this mutual-information-driven objective highlights the need to normalize the raw activation with $p(\mathbf{w}_m|w)$. That is, if a word whose output embedding consistently activates various feature vectors, it loses specification for interpretation.

4 Evaluation Metrics and Methods

Evaluating SAEs is inherently challenging due to the absence of ground truth labels. Unlike traditional machine learning tasks where performance

can be directly measured against labeled data, the quality of an SAE must be inferred through a diverse set of metrics. These metrics assess both the internal structure of the model and its functional utility. To provide a comprehensive evaluation framework, we categorize SAE evaluation methods into two main groups: structural metrics and functional metrics. This categorization ensures a holistic assessment of SAEs, covering both their training behavior and real-world applicability.

4.1 Structural Metrics

Structural metrics focus on assessing whether an SAE behaves as intended during training. SAEs are designed to optimize both reconstruction fidelity and sparsity, as these properties are explicitly enforced in the training loss. Therefore, natural evaluation metrics assess reconstruction accuracy and sparsity in the model's learned representations.

Reconstruction Fidelity. The most fundamental way to evaluate reconstruction fidelity is through Mean Squared Error (MSE) and Cosine Similarity (Ng et al., 2011), which directly compare the original activations with SAE-reconstructed activations. Additional metrics such as Fraction of Variance Unexplained (FVU) (also known as normalized loss) (Gao et al., 2025) and Explained Variance (Karvonen et al., 2024) measure how much variance in the original data is retained after SAE reconstructs. Beyond direct reconstruction comparisons, researchers also evaluate how SAEs affect the probability distribution of model outputs. Cross-Entropy Loss (Shannon, 1948) and KL Divergence (Kullback and Leibler, 1951) measure the shift in probability distributions when substituting original model activations with SAE-generated activations. If the SAE faithfully reconstructs activations, the probability distributions should remain similar. Similarly, Delta LM Loss (Lieberum et al., 2024) quantifies the difference between the original language model loss and the loss incurred when replacing activations with those from the SAE. Another important aspect of reconstruction fidelity is magnitude preservation. The L2 Ratio (Karvonen et al., 2024) compares the Euclidean norms of different activations to ensure that the SAE does not systematically alter activation magnitudes.

Sparsity. A key design objective of SAEs is sparsity, which ensures that only a small subset of latent neurons activate for any given input. The most direct metric for sparsity is L0 Sparsity (Louizos et al., 2017), which measures the average number of nonzero activations per input. However, sparsity is not just about minimizing activations; it also requires ensuring that the active features are meaningful. To assess feature usage patterns, Latent Firing Frequency (He et al., 2024) and Feature Density Statistics (Karvonen et al., 2024) track how often each SAE latent is activated across different inputs, ensuring that features are neither too frequent nor inactive. Additionally, the Sparsity-fidelity Tradeoff (Gao et al., 2025) evaluates whether adjusting sparsity affects reconstruction quality, helping to determine the optimal balance between sparsity and fidelity.

4.2 Functional Metrics

While structural metrics ensure that an SAE follows its design principles, functional metrics assess whether the SAE is useful for real-world analysis. These include interpretability, which assesses whether the SAE's learned features correspond to meaningful and distinct concepts, and robustness, which evaluates whether the learned representations are stable and generalizable.

Interpretability. One of the primary motivations for SAEs is to enhance interpretability by disentangling LLM activations into meaningful features. A crucial property for interpretability is monosemanticity, where each feature should encode a single concept. RAVEL and Automated Interpretability (Karvonen et al., 2024) automatically evaluate monosemanticity by using a language model to generate and assess feature descriptions. These methods analyze the most activating contexts for each feature and assign interpretability scores. Sparse Probing and Targeted Probe Perturbation (TPP) (Karvonen et al., 2024) evaluate whether SAE features align with specific downstream tasks. In sparse probing, a linear probe is trained using only a small subset of SAE activations, while TPP measures how much perturbing individual latents impacts probe accuracy. If a small number of active features enable strong performance, the SAE has learned disentangled and meaningful representations. Beyond evaluating feature alignment, it is also crucial to assess the faithfulness of feature descriptions. Input-Based Evaluation and Output-Based Evaluation (Gur-Arieh et al., 2025) provide a framework for verifying whether feature descriptions accurately reflect what a feature represents. Input-Based Evaluation tests whether a given feature description correctly identifies which inputs activate the feature by generating activating and

neutral examples and measuring activation differences. Output-Based Evaluation assesses whether a feature description captures the causal influence of the feature on model outputs by modifying feature activations and comparing the resulting generated texts. Feature Absorption (Karvonen et al., 2024) assesses whether a feature is capturing multiple independent concepts instead of a single interpretable concept. If adding more features does not significantly improve representation quality, it suggests that the extracted features are already sufficient. Another approach to detecting whether each neuron is monosemantic is checking for redundancy or overlap with other neurons. Feature Geometry Analysis (He et al., 2024; Bricken et al., 2023; Templeton et al., 2024) detects redundancy among SAE latents by measuring cosine similarity between decoder columns. If two features have high cosine similarity, they may represent redundant concepts rather than independent units.

Robustness. In addition to being interpretable, a well-designed SAE should be robust in various contexts. Robustness ensures that SAEs do not overfit to a specific dataset or condition but instead generalize effectively. Generalizability (He et al., 2024) assesses whether SAEs remain effective when applied to out-of-distribution data. Two common tests for generalizability include evaluating whether SAEs trained on shorter text sequences still perform well on longer sequences and checking whether SAEs trained on base LLM activations generalize to instruction-finetuned models. Unlearning (Karvonen et al., 2024) measures whether an SAE can selectively forget specific features while preserving useful information. This is crucial for applications that require privacy-focused models, where sensitive information needs to be erased. Spurious Correlation Removal (SCR) (Karvonen et al., 2024) tests whether an SAE can eliminate biased correlations in downstream models. If removing certain latents reduces unwanted correlations without harming performance, the SAE has learned to capture and remove spurious patterns.

Moreover, we provide a comprehensive comparison of SAEs using both structural and functional metrics in Appendix D.

5   Applications in Large Language Models

The latents learned by SAEs represent a collection of low-level concepts. Each SAE latent can be interpreted through gathering its activating examples (Lin, 2023). This approach enables latents to be interpreted in a human-understandable manner, thereby enhancing our comprehension of how models perform tasks and facilitating more effective control of model behaviors.

5.1   Model Steering

Unlike supervised concept vectors, such as probing classifiers (Belinkov, 2022; Zhao et al., 2025; Jin et al., 2025), SAEs can simultaneously learn a large volume of concept vectors. The learned vectors can then be utilized to steer model behaviors in ways similar to supervised vectors (See Figure 3). A detailed comparison between SAEs and probing-based methods is provided in Appendix F.

As previously mentioned, SAE latents can be employed to produce steering vectors that control model outputs related to toxicity, sycophancy, refusal, and emotions. Other steering applications have also proven feasible. Recently, a study shows that SAE latents are able to capture instructions such as translations. These identified latents are effective in manipulating models to translate inputs according to specific instructions (He et al., 2025). Another investigation focusing on semantic search demonstrates that SAEs can learn fine-grained semantic concepts at various levels of abstraction. These concept vectors can be used to steer models toward related semantic (O'Neill et al., 2024). Alternatively, SAEs trained on biological datasets can provide biology-related features that enable the unlearning of biology-relevant knowledge with fewer side effects than existing techniques (Farrell et al., 2024). Given that steering effects are generally challenging to control, SAE-TS further utilizes SAE latents to optimize steering vectors by measuring the changes in SAE feature activation caused by steering, thereby helping construct vectors that target relevant features while minimizing unwanted effects (Chalnev et al., 2024). Moreover, explanations based on SAE latents risk prioritizing linguistic features over semantic meaning. Wu et al. (2025b) propose a novel approach that promotes diverse semantic explanations, which has been demonstrated to enhance model safety.

5.2   Model Behavior Analysis

SAEs construct a dictionary of concepts through their latents, providing a more fine-grained perspective for concept interpretation. This capability enables the analysis of the model's internal representations and learned knowledge in greater detail.
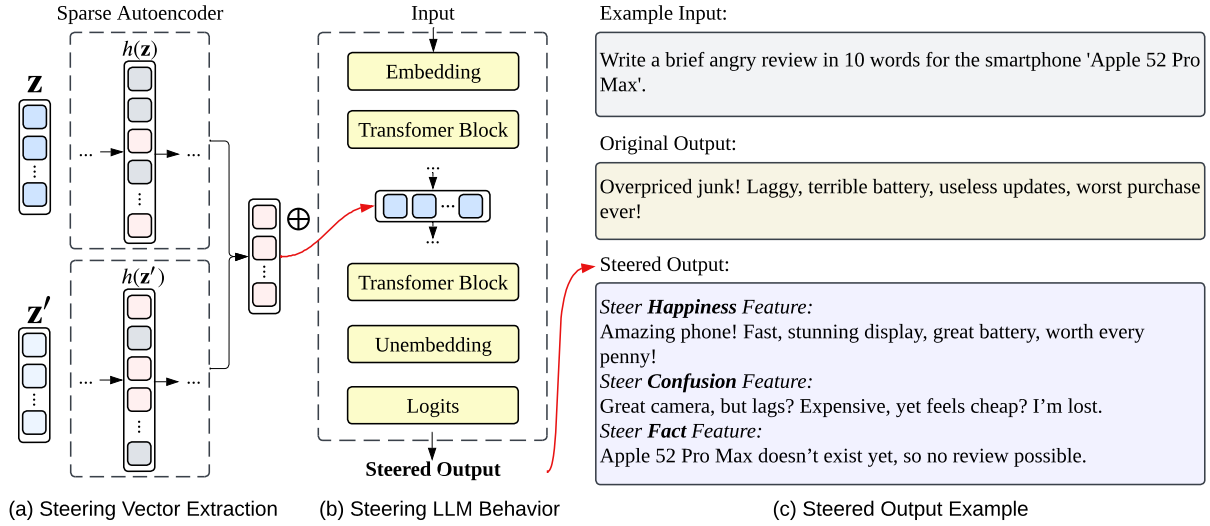
Figure 3: The figure illustrates the process of using a SAE to steer the behavior of a LLM, with an example of the resulting steered output. In part (a), normally people use SAE to extract a steering vector by comparing two representations: $\mathbf{z}$, which lacks a certain feature, and $\mathbf{z}'$, which contains that feature. In part (b), this steering vector is added to the input representation, modifying the LLM's behavior to align with the desired feature. Part (c) demonstrates the example results of this process, where the steered output reflects the steered feature, even when the original input prompt is neutral or contradictory to the feature being introduced.

A recent study utilizes SAEs to reveal the mechanism of hallucination, where entity recognition plays a pivot role in recalling facts. A direction distinguishing whether the model knows an entity is identified, which is usually used for hallucination refusal in chat models (Ferrando et al., 2025). Some studies focus on interpreting how in-context learning (ICL) is performed within models. One study focuses on general ICL tasks, and task-related function vectors were successfully isolated (Kharlapenko et al., 2024). Another study focuses on reinforcement learning (RL) tasks. Their experiment shows that an LLM's internal representations are capable of capturing temporal difference errors and Q-values that are essential in RL computations (Demircan et al., 2025). Besides, one study attempts to examine the working mechanism of instruction following. Their analysis on translation tasks shows that instructions are composed of multiple relevant concepts rather than individual ones (He et al., 2025).

Moreover, SAEs have been employed to study behaviors related to toxicity, sycophancy, refusal, and emotions. One recent study shows that features captured by SAEs can be used to construct probes to classify cross-lingual toxicity (Gallifant et al., 2025). By examining SAE latents that activate on anger-related tokens, researchers have identified steering vectors that control angry out-

puts (Nanda et al., 2024). Additionally, other research demonstrates that SAEs can reconstruct vectors responsible for refusing to answer harmful questions as well as directions that produce sycophantic responses (neverix et al., 2024). Please refer to Appendix E for more LLM applications.

6 Conclusions

In this survey, we provided a comprehensive examination of SAEs as a promising approach to interpreting and understanding LLMs. SAEs effectively address the challenge of polysemanticity through learning overcomplete, sparse representations that disentangle superimposed features into more interpretable units. We have systematically explored the foundational principles, technical frameworks, evaluation methodologies, and real-world applications of SAEs in the context of LLM analysis. While SAEs have demonstrated considerable success in revealing the internal mechanisms of LLMs, several challenges remain. In Appendix G, we discussed detailed research challenges, including the incompleteness of concept dictionaries, limited theoretical foundations, persistent reconstruction errors, and substantial computational requirements. Despite these challenges, SAEs continue to evolve through architectural innovations and improved training strategies, offering deeper insights into the inner workings of complex LLMs.

Limitations

Many concepts central to SAEs, such as polysemanticity, superposition, and feature disentanglement, have been extensively studied under different frameworks including distributed representations, disentangled representation learning, and sparse coding in computer vision and signal processing. This paper focuses specifically on introducing SAEs during the LLM era, examining their applications in interpreting transformer-based language models, and does not extensively cover these concepts' history in adjacent fields.

Acknowledgments

References

Anthropic. 2024. [link].

Anthropic. 2024. Introducing Claude 3.5 Sonnet. Announcement of Claude 3.5 Sonnet model release, featuring improved intelligence, vision capabilities, and new Artifacts feature.

Sanjeev Arora, Yuanzhi Li, Yingyu Liang, Tengyu Ma, and Andrej Risteski. 2018. Linear algebraic structure of word senses, with applications to polysemy. *Transactions of the Association for Computational Linguistics*, 6:483–495.

Kola Ayonrinde. 2024. Adaptive sparse allocation with mutual choice & feature choice sparse autoencoders. *arXiv preprint arXiv:2411.02124*.

Yonatan Belinkov. 2022. Probing classifiers: Promises, shortcomings, and advances. *Computational Linguistics*, 48(1):207–219.

Leonard Bereska and Efstratios Gavves. 2024a. Mechanistic interpretability for ai safety–a review. *arXiv preprint arXiv:2404.14082*.

Leonard Bereska and Stratis Gavves. 2024b. Mechanistic interpretability for ai safety-a review. *Transactions on Machine Learning Research*.

Stella Biderman, Hailey Schoelkopf, Quentin Gregory Anthony, Herbie Bradley, Kyle O'Brien, Eric Hallahan, Mohammad Aflah Khan, Shivanshu Purohit, USVSN Sai Prashanth, Edward Raff, et al. 2023. Pythia: A suite for analyzing large language models across training and scaling. In *International Conference on Machine Learning*, pages 2397–2430. PMLR.

Steven Bills, Nick Cammarata, Dan Mossing, Henk Tillman, Leo Gao, Gabriel Goh, Ilya Sutskever, Jan Leike, Jeff Wu, and William Saunders. 2023. Language models can explain neurons in language models. https://openaipublic.blob.core.windows.net/neuron-explainer/paper/index.html.

Joseph Bloom. 2024. Open source sparse autoencoders for all residual stream layers of gpt2 small.

Dan Braun, Jordan Taylor, Nicholas Goldowsky-Dill, and Lee Sharkey. 2025. Identifying functionally important features with end-to-end sparse dictionary learning. *Advances in Neural Information Processing Systems*, 37:107286–107325.

Trenton Bricken, Adly Templeton, Joshua Batson, Brian Chen, Adam Jermyn, Tom Conerly, Nick Turner, Cem Anil, Carson Denison, Amanda Askell, Robert Lasenby, Yifan Wu, Shauna Kravec, Nicholas Schiefer, Tim Maxwell, Nicholas Joseph, Zac Hatfield-Dodds, Alex Tamkin, Karina Nguyen, Brayden McLean, Josiah E Burke, Tristan Hume, Shan Carter, Tom Henighan, and Christopher Olah. 2023. Towards monosemanticity: Decomposing language models with dictionary learning. *Transformer Circuits Thread*. Https://transformer-circuits.pub/2023/monosemantic-features/index.html.

Bart Bussmann, Patrick Leask, and Neel Nanda. 2024. Batchtopk sparse autoencoders. *arXiv preprint arXiv:2412.06410*.

Sviatoslav Chalnev, Matthew Siu, and Arthur Conmy. 2024. Improving steering vectors by targeting sparse autoencoder features. *arXiv preprint arXiv:2411.02193*.

Thomas M Cover. 1999. *Elements of information theory*. John Wiley & Sons.

Hoagy Cunningham, Aidan Ewart, Logan Riggs, Robert Huben, and Lee Sharkey. 2023. Sparse autoencoders find highly interpretable features in language models. *arXiv preprint arXiv:2309.08600*.

Yann N Dauphin, Angela Fan, Michael Auli, and David Grangier. 2017. Language modeling with gated convolutional networks. In *International conference on machine learning*, pages 933–941. PMLR.

DeepSeek-AI, Daya Guo, Dejian Yang, Haowei Zhang, Junxiao Song, Ruoyu Zhang, Runxin Xu, Qihao Zhu, Shirong Ma, Peiyi Wang, Xiao Bi, Xiaokang Zhang, Xingkai Yu, Yu Wu, Z. F. Wu, Zhibin Gou, Zhihong Shao, Zhuoshu Li, Ziyi Gao, Aixin Liu, Bing Xue, Bingxuan Wang, Bochao Wu, Bei Feng, Chengda Lu, Chenggang Zhao, Chengqi Deng, Chenyu Zhang, Chong Ruan, Damai Dai, Deli Chen, Dongjie Ji, Erhang Li, Fangyun Lin, Fucong Dai, Fuli Luo, Guangbo Hao, Guanting Chen, Guowei Li, H. Zhang,

Han Bao, Hanwei Xu, Haocheng Wang, Honghui Ding, Huajian Xin, Huazuo Gao, Hui Qu, Hui Li, Jianzhong Guo, Jiashi Li, Jiawei Wang, Jingchang Chen, Jingyang Yuan, Junjie Qiu, Junlong Li, J. L. Cai, Jiaqi Ni, Jian Liang, Jin Chen, Kai Dong, Kai Hu, Kaige Gao, Kang Guan, Kexin Huang, Kuai Yu, Lean Wang, Lecong Zhang, Liang Zhao, Litong Wang, Liyue Zhang, Lei Xu, Leyi Xia, Mingchuan Zhang, Minghua Zhang, Minghui Tang, Meng Li, Miaojun Wang, Mingming Li, Ning Tian, Panpan Huang, Peng Zhang, Qiancheng Wang, Qinyu Chen, Qiushi Du, Ruiqi Ge, Ruisong Zhang, Ruizhe Pan, Runji Wang, R. J. Chen, R. L. Jin, Ruyi Chen, Shanghao Lu, Shangyan Zhou, Shanhuang Chen, Shengfeng Ye, Shiyu Wang, Shuiping Yu, Shunfeng Zhou, Shuting Pan, S. S. Li, Shuang Zhou, Shaoqing Wu, Shengfeng Ye, Tao Yun, Tian Pei, Tianyu Sun, T. Wang, Wangding Zeng, Wanjia Zhao, Wen Liu, Wenfeng Liang, Wenjun Gao, Wenqin Yu, Wentao Zhang, W. L. Xiao, Wei An, Xiaodong Liu, Xiaohan Wang, Xiaokang Chen, Xiaotao Nie, Xin Cheng, Xin Liu, Xin Xie, Xingchao Liu, Xinyu Yang, Xinyuan Li, Xuecheng Su, Xuheng Lin, X. Q. Li, Xiangyue Jin, Xiaojin Shen, Xiaosha Chen, Xiaowen Sun, Xiaoxiang Wang, Xinnan Song, Xinyi Zhou, Xianzu Wang, Xinxia Shan, Y. K. Li, Y. Q. Wang, Y. X. Wei, Yang Zhang, Yanhong Xu, Yao Li, Yao Zhao, Yaofeng Sun, Yaohui Wang, Yi Yu, Yichao Zhang, Yifan Shi, Yiliang Xiong, Ying He, Yishi Piao, Yisong Wang, Yixuan Tan, Yiyang Ma, Yiyuan Liu, Yongqiang Guo, Yuan Ou, Yuduan Wang, Yue Gong, Yuheng Zou, Yujia He, Yunfan Xiong, Yuxiang Luo, Yuxiang You, Yuxuan Liu, Yuyang Zhou, Y. X. Zhu, Yanhong Xu, Yanping Huang, Yaohui Li, Yi Zheng, Yuchen Zhu, Yunxian Ma, Ying Tang, Yukun Zha, Yuting Yan, Z. Z. Ren, Zehui Ren, Zhangli Sha, Zhe Fu, Zhean Xu, Zhenda Xie, Zhengyan Zhang, Zhewen Hao, Zhicheng Ma, Zhigang Yan, Zhiyu Wu, Zihui Gu, Zijia Zhu, Zijun Liu, Zilin Li, Ziwei Xie, Ziyang Song, Zizheng Pan, Zhen Huang, Zhipeng Xu, Zhongyu Zhang, and Zhen Zhang. 2025. Deepseek-r1: Incentivizing reasoning capability in llms via reinforcement learning. *Preprint*, arXiv:2501.12948.

Can Demircan, Tankred Saanum, Akshay Kumar Jagadish, Marcel Binz, and Eric Schulz. 2025. Sparse autoencoders reveal temporal difference learning in large language models. In *The Thirteenth International Conference on Learning Representations*.

Jonathan Donnelly and Adam Roegiest. 2019. On interpretability and feature representations: an analysis of the sentiment neuron. In *Advances in Information Retrieval: 41st European Conference on IR Research, ECIR 2019, Cologne, Germany, April 14–18, 2019, Proceedings, Part I 41*, pages 795–802. Springer.

Abhimanyu Dubey, Abhinav Jauhri, Abhinav Pandey, Abhishek Kadian, Ahmad Al-Dahle, Aiesha Letman, Akhil Mathur, Alan Schelten, Amy Yang, Angela Fan, et al. 2024. The llama 3 herd of models. *arXiv preprint arXiv:2407.21783*.

Nelson Elhage, Tristan Hume, Catherine Olsson, Nicholas Schiefer, Tom Henighan, Shauna Kravec, Zac Hatfield-Dodds, Robert Lasenby, Dawn Drain, Carol Chen, Roger Grosse, Sam McCandlish, Jared Kaplan, Dario Amodei, Martin Wattenberg, and Christopher Olah. 2022. Toy models of superposition. *Transformer Circuits Thread*.

Eoin Farrell, Yeu-Tong Lau, and Arthur Conmy. 2024. Applying sparse autoencoders to unlearn knowledge in language models. In *Neurips Safe Generative AI Workshop 2024*.

Manaal Faruqui, Yulia Tsvetkov, Dani Yogatama, Chris Dyer, and Noah Smith. 2015. Sparse overcomplete word vector representations. *arXiv preprint arXiv:1506.02004*.

Javier Ferrando, Oscar Balcells Obeso, Senthooran Rajamanoharan, and Neel Nanda. 2025. Do i know this entity? knowledge awareness and hallucinations in language models. In *The Thirteenth International Conference on Learning Representations*.

Javier Ferrando, Gabriele Sarti, Arianna Bisazza, and Marta R Costa-jussà. 2024. A primer on the inner workings of transformer-based language models. *arXiv preprint arXiv:2405.00208*.

Alex Foote, Neel Nanda, Esben Kran, Ioannis Konstas, Shay Cohen, and Fazl Barez. 2023. Neuron to graph: Interpreting language model neurons at scale. *arXiv preprint arXiv:2305.19911*.

Andrey Galichin, Alexey Dontsov, Polina Druzhinina, Anton Razzhigaev, Oleg Y Rogov, Elena Tutubalina, and Ivan Oseledets. 2025. I have covered all the bases here: Interpreting reasoning features in large language models via sparse autoencoders. *arXiv preprint arXiv:2503.18878*.

Jack Gallifant, Shan Chen, Kuleen Sasse, Hugo Aerts, Thomas Hartvigsen, and Danielle S Bitterman. 2025. Sparse autoencoder features for classifications and transferability. *arXiv preprint arXiv:2502.11367*.

Jun Gao, Di He, Xu Tan, Tao Qin, Liwei Wang, and Tie-Yan Liu. 2019. Representation degeneration problem in training natural language generation models. *arXiv preprint arXiv:1907.12009*.

Leo Gao, Tom Dupre la Tour, Henk Tillman, Gabriel Goh, Rajan Troll, Alec Radford, Ilya Sutskever, Jan Leike, and Jeffrey Wu. 2025. Scaling and evaluating sparse autoencoders. In *The Thirteenth International Conference on Learning Representations*.

Atticus Geiger, Duligur Ibeling, Amir Zur, Maheep Chaudhary, Sonakshi Chauhan, Jing Huang, Aryaman Arora, Zhengxuan Wu, Noah Goodman, Christopher Potts, et al. 2023. Causal abstraction: A theoretical foundation for mechanistic interpretability. *arXiv preprint arXiv:2301.04709*.

Davide Ghilardi, Federico Belotti, and Marco Molinari. 2024. Efficient training of sparse autoencoders for large language models via layer groups. *arXiv preprint arXiv:2410.21508*.

Mario Giulianelli, Jacqueline Harding, Florian Mohnert, Dieuwke Hupkes, and Willem Zuidema. 2018. Under the hood: Using diagnostic classifiers to investigate and improve how language models track agreement information. *arXiv preprint arXiv:1808.08079*.

Karol Gregor and Yann LeCun. 2010. Learning fast approximations of sparse coding. In *Proceedings of the 27th international conference on international conference on machine learning*, pages 399–406.

Clément Guerner, Anej Svete, Tianyu Liu, Alexander Warstadt, and Ryan Cotterell. 2023. A geometric notion of causal probing. *arXiv preprint arXiv:2307.15054*.

Yoav Gur-Arieh, Roy Mayan, Chen Agassy, Atticus Geiger, and Mor Geva. 2025. Enhancing automated interpretability with output-centric feature descriptions. *arXiv preprint arXiv:2501.08319*.

Zhengfu He, Wentao Shu, Xuyang Ge, Lingjie Chen, Junxuan Wang, Yunhua Zhou, Frances Liu, Qipeng Guo, Xuanjing Huang, Zuxuan Wu, et al. 2024. Llama scope: Extracting millions of features from llama-3.1-8b with sparse autoencoders. *arXiv preprint arXiv:2410.20526*.

Zirui He, Haiyan Zhao, Yiran Qiao, Fan Yang, Ali Payani, Jing Ma, and Mengnan Du. 2025. Saif: A sparse autoencoder framework for interpreting and steering instruction following of language models. *arXiv preprint arXiv:2502.11356*.

Irina Higgins, David Amos, David Pfau, Sebastien Racaniere, Loic Matthey, Danilo Rezende, and Alexander Lerchner. 2018. Towards a definition of disentangled representations. *arXiv preprint arXiv:1812.02230*.

Geoffrey E Hinton. 1984. Distributed representations.

Mingyu Jin, Qinkai Yu, Jingyuan Huang, Qingcheng Zeng, Zhenting Wang, Wenyue Hua, Haiyan Zhao, Kai Mei, Yanda Meng, Kaize Ding, et al. 2025. Exploring concept depth: How large language models acquire knowledge and concept at different layers? In *Proceedings of the 31st International Conference on Computational Linguistics*, pages 558–573.

Subhash Kantamneni, Joshua Engels, Senthooran Rajamanoharan, Max Tegmark, and Neel Nanda. 2025. Are sparse autoencoders useful? a case study in sparse probing. *Preprint*, arXiv:2502.16681.

A Karvonen, C Rager, J Lin, C Tigges, J Bloom, D Chanin, YT Lau, E Farrell, A Conmy, C McDougall, et al. 2024. Saebench: A comprehensive benchmark for sparse autoencoders, december 2024. *URL https://www. neuronpedia. org/sae-bench/info*.

Dmitrii Kharlapenko, neverix, Neel Nanda, and Authur Conmy. 2024. Extracting SAE task features for in-context learning. [Accessed 26-02-2025].

Been Kim, Martin Wattenberg, Justin Gilmer, Carrie Cai, James Wexler, Fernanda Viegas, et al. 2018. Interpretability beyond feature attribution: Quantitative testing with concept activation vectors (tcav). In *International conference on machine learning*, pages 2668–2677. PMLR.

Hyunjik Kim and Andriy Mnih. 2018. Disentangling by factorising. In *International conference on machine learning*, pages 2649–2658. PMLR.

Solomon Kullback and Richard A Leibler. 1951. On information and sufficiency. *The annals of mathematical statistics*, 22(1):79–86.

Justin Lee, Tuomas Oikarinen, Arjun Chatha, Keng-Chi Chang, Yilan Chen, and Tsui-Wei Weng. 2023. The importance of prompt tuning for automated neuron explanations. *arXiv preprint arXiv:2310.06200*.

Tom Lieberum, Senthooran Rajamanoharan, Arthur Conmy, Lewis Smith, Nicolas Sonnerat, Vikrant Varma, János Kramár, Anca Dragan, Rohin Shah, and Neel Nanda. 2024. Gemma scope: Open sparse autoencoders everywhere all at once on gemma 2. *arXiv preprint arXiv:2408.05147*.

Johnny Lin. 2023. Neuronpedia: Interactive reference and tooling for analyzing neural networks. Software available from neuronpedia.org.

Francesco Locatello, Stefan Bauer, Mario Lucic, Gunnar Raetsch, Sylvain Gelly, Bernhard Schölkopf, and Olivier Bachem. 2019. Challenging common assumptions in the unsupervised learning of disentangled representations. In *international conference on machine learning*, pages 4114–4124. PMLR.

Christos Louizos, Max Welling, and Diederik P Kingma. 2017. Learning sparse neural networks through l_0 regularization. *arXiv preprint arXiv:1712.01312*.

Luke Marks, Alasdair Paren, David Krueger, and Fazl Barez. 2024. Enhancing neural network interpretability with feature-aligned sparse autoencoders. *arXiv preprint arXiv:2411.01220*.

Kevin Meng, David Bau, Alex Andonian, and Yonatan Belinkov. 2022. Locating and editing factual associations in gpt. *Advances in neural information processing systems*, 35:17359–17372.

Abhinav Menon, Manish Shrivastava, David Krueger, and Ekdeep Singh Lubana. 2024. Analyzing (in) abilities of saes via formal languages. *arXiv preprint arXiv:2410.11767*.

Tomas Mikolov, Ilya Sutskever, Kai Chen, Greg S Corrado, and Jeff Dean. 2013a. Distributed representations of words and phrases and their compositionality. *Advances in neural information processing systems*, 26.

Tomáš Mikolov, Wen-tau Yih, and Geoffrey Zweig. 2013b. Linguistic regularities in continuous space word representations. In *Proceedings of the 2013*

conference of the north american chapter of the association for computational linguistics: Human language technologies, pages 746–751.

Anish Mudide, Joshua Engels, Eric J Michaud, Max Tegmark, and Christian Schroeder de Witt. 2024. Efficient dictionary learning with switch sparse autoencoders. *arXiv preprint arXiv:2410.08201*.

Aashiq Muhamed, Mona Diab, and Virginia Smith. 2024. Decoding dark matter: Specialized sparse autoencoders for interpreting rare concepts in foundation models. *arXiv preprint arXiv:2411.00743*.

Neel Nanda, Arthur Conmy, Lewis Smith, Senthooran Rajamanoharan, Tom Lieberum, János Kramár, and Vikrant Varma. 2024. [Full Post] Progress Update #1 from the GDM Mech Interp Team. [Accessed 26-02-2025].

Neel Nanda, Andrew Lee, and Martin Wattenberg. 2023. Emergent linear representations in world models of self-supervised sequence models. *arXiv preprint arXiv:2309.00941*.

neverix, Dmitrii Kharlapenko, Arthur Conmy, and Neel Nanda. 2024. SAE features for refusal and sycophancy steering vectors. [Accessed 26-02-2025].

Andrew Ng et al. 2011. Sparse autoencoder. *CS294A Lecture notes*, 72(2011):1–19.

Anh Nguyen, Jason Yosinski, and Jeff Clune. 2019. Understanding neural networks via feature visualization: A survey. *Explainable AI: interpreting, explaining and visualizing deep learning*, pages 55–76.

Angus Nicolson, Lisa Schut, J Alison Noble, and Yarin Gal. 2024. Explaining explainability: Understanding concept activation vectors. *arXiv preprint arXiv:2404.03713*.

Nostalgebraist. 2020. Interpreting gpt: the logit lens.

Chris Olah. 2023. Distributed representations: Composition & superposition. *Transformer Circuits Thread*, 27.

Bruno A Olshausen and David J Field. 1997. Sparse coding with an overcomplete basis set: A strategy employed by v1? *Vision research*, 37(23):3311–3325.

Charles O'Neill, Christine Ye, Kartheik Iyer, and John F Wu. 2024. Disentangling dense embeddings with sparse autoencoders. *arXiv preprint arXiv:2408.00657*.

OpenAI, Josh Achiam, Steven Adler, Sandhini Agarwal, Lama Ahmad, Ilge Akkaya, Florencia Leoni Aleman, Diogo Almeida, Janko Altenschmidt, Sam Altman, Shyamal Anadkat, Red Avila, Igor Babuschkin, Suchir Balaji, Valerie Balcom, Paul Baltescu, Haiming Bao, Mohammad Bavarian, Jeff Belgum, Irwan Bello, Jake Berdine, Gabriel Bernadett-Shapiro, Christopher Berner, Lenny Bogdonoff, Oleg Boiko, Madelaine Boyd, Anna-Luisa Brakman, Greg Brockman, Tim Brooks, Miles Brundage, Kevin Button, Trevor Cai, Rosie Campbell, Andrew Cann, Brittany Carey, Chelsea Carlson, Rory Carmichael, Brooke Chan, Che Chang, Fotis Chantzis, Derek Chen, Sully Chen, Ruby Chen, Jason Chen, Mark Chen, Ben Chess, Chester Cho, Casey Chu, Hyung Won Chung, Dave Cummings, Jeremiah Currier, Yunxing Dai, Cory Decareaux, Thomas Degry, Noah Deutsch, Damien Deville, Arka Dhar, David Dohan, Steve Dowling, Sheila Dunning, Adrien Ecoffet, Atty Eleti, Tyna Eloundou, David Farhi, Liam Fedus, Niko Felix, Simón Posada Fishman, Juston Forte, Isabella Fulford, Leo Gao, Elie Georges, Christian Gibson, Vik Goel, Tarun Gogineni, Gabriel Goh, Rapha Gontijo-Lopes, Jonathan Gordon, Morgan Grafstein, Scott Gray, Ryan Greene, Joshua Gross, Shixiang Shane Gu, Yufei Guo, Chris Hallacy, Jesse Han, Jeff Harris, Yuchen He, Mike Heaton, Johannes Heidecke, Chris Hesse, Alan Hickey, Wade Hickey, Peter Hoeschele, Brandon Houghton, Kenny Hsu, Shengli Hu, Xin Hu, Joost Huizinga, Shantanu Jain, Shawn Jain, Joanne Jang, Angela Jiang, Roger Jiang, Haozhun Jin, Denny Jin, Shino Jomoto, Billie Jonn, Heewoo Jun, Tomer Kaftan, Łukasz Kaiser, Ali Kamali, Ingmar Kanitscheider, Nitish Shirish Keskar, Tabarak Khan, Logan Kilpatrick, Jong Wook Kim, Christina Kim, Yongjik Kim, Jan Hendrik Kirchner, Jamie Kiros, Matt Knight, Daniel Kokotajlo, Łukasz Kondraciuk, Andrew Kondrich, Aris Konstantinidis, Kyle Kosic, Gretchen Krueger, Vishal Kuo, Michael Lampe, Ikai Lan, Teddy Lee, Jan Leike, Jade Leung, Daniel Levy, Chak Ming Li, Rachel Lim, Molly Lin, Stephanie Lin, Mateusz Litwin, Theresa Lopez, Ryan Lowe, Patricia Lue, Anna Makanju, Kim Malfacini, Sam Manning, Todor Markov, Yaniv Markovski, Bianca Martin, Katie Mayer, Andrew Mayne, Bob McGrew, Scott Mayer McKinney, Christine McLeavey, Paul McMillan, Jake McNeil, David Medina, Aalok Mehta, Jacob Menick, Luke Metz, Andrey Mishchenko, Pamela Mishkin, Vinnie Monaco, Evan Morikawa, Daniel Mossing, Tong Mu, Mira Murati, Oleg Murk, David Mély, Ashvin Nair, Reiichiro Nakano, Rajeev Nayak, Arvind Neelakantan, Richard Ngo, Hyeonwoo Noh, Long Ouyang, Cullen O'Keefe, Jakub Pachocki, Alex Paino, Joe Palermo, Ashley Pantuliano, Giambattista Parascandolo, Joel Parish, Emy Parparita, Alex Passos, Mikhail Pavlov, Andrew Peng, Adam Perelman, Filipe de Avila Belbute Peres, Michael Petrov, Henrique Ponde de Oliveira Pinto, Michael, Pokorny, Michelle Pokrass, Vitchyr H. Pong, Tolly Powell, Alethea Power, Boris Power, Elizabeth Proehl, Raul Puri, Alec Radford, Jack Rae, Aditya Ramesh, Cameron Raymond, Francis Real, Kendra Rimbach, Carl Ross, Bob Rotsted, Henri Roussez, Nick Ryder, Mario Saltarelli, Ted Sanders, Shibani Santurkar, Girish Sastry, Heather Schmidt, David Schnurr, John Schulman, Daniel Selsam, Kyla Sheppard, Toki Sherbakov, Jessica Shieh, Sarah Shoker, Pranav Shyam, Szymon Sidor, Eric Sigler, Maddie Simens, Jordan Sitkin, Katarina Slama, Ian Sohl, Benjamin Sokolowsky, Yang Song, Natalie Staudacher, Felipe Petroski Such, Natalie Summers, Ilya Sutskever,

Jie Tang, Nikolas Tezak, Madeleine B. Thompson, Phil Tillet, Amin Tootoonchian, Elizabeth Tseng, Preston Tuggle, Nick Turley, Jerry Tworek, Juan Felipe Cerón Uribe, Andrea Vallone, Arun Vijayvergiya, Chelsea Voss, Carroll Wainwright, Justin Jay Wang, Alvin Wang, Ben Wang, Jonathan Ward, Jason Wei, CJ Weinmann, Akila Welihinda, Peter Welinder, Jiayi Weng, Lilian Weng, Matt Wiethoff, Dave Willner, Clemens Winter, Samuel Wolrich, Hannah Wong, Lauren Workman, Sherwin Wu, Jeff Wu, Michael Wu, Kai Xiao, Tao Xu, Sarah Yoo, Kevin Yu, Qiming Yuan, Wojciech Zaremba, Rowan Zellers, Chong Zhang, Marvin Zhang, Shengjia Zhao, Tianhao Zheng, Juntang Zhuang, William Zhuk, and Barret Zoph. 2024. Gpt-4 technical report. *Preprint*, arXiv:2303.08774.

Kiho Park, Yo Joong Choe, and Victor Veitch. 2023. The linear representation hypothesis and the geometry of large language models. *arXiv preprint arXiv:2311.03658*.

Jeffrey Pennington, Richard Socher, and Christopher D Manning. 2014. Glove: Global vectors for word representation. In *Proceedings of the 2014 conference on empirical methods in natural language processing (EMNLP)*, pages 1532–1543.

Alec Radford, Rafal Jozefowicz, and Ilya Sutskever. 2017. Learning to generate reviews and discovering sentiment. *arXiv preprint arXiv:1704.01444*.

Alec Radford, Jeffrey Wu, Rewon Child, David Luan, Dario Amodei, Ilya Sutskever, et al. 2019. Language models are unsupervised multitask learners. *OpenAI blog*, 1(8):9.

Daking Rai, Yilun Zhou, Shi Feng, Abulhair Saparov, and Ziyu Yao. 2024. A practical review of mechanistic interpretability for transformer-based language models. *arXiv preprint arXiv:2407.02646*.

Senthooran Rajamanoharan, Arthur Conmy, Lewis Smith, Tom Lieberum, Vikrant Varma, János Kramár, Rohin Shah, and Neel Nanda. 2024a. Improving dictionary learning with gated sparse autoencoders. *arXiv preprint arXiv:2404.16014*.

Senthooran Rajamanoharan, Tom Lieberum, Nicolas Sonnerat, Arthur Conmy, Vikrant Varma, János Kramár, and Neel Nanda. 2024b. Jumping ahead: Improving reconstruction fidelity with jumprelu sparse autoencoders. *arXiv preprint arXiv:2407.14435*.

Marks Samuel, Karvonen Adam, and Mueller Aaron. 2024. dictionary learning. https://github.com/saprmarks/dictionary_learning.

Naomi Saphra and Sarah Wiegreffe. 2024. Mechanistic? *arXiv preprint arXiv:2410.09087*.

Claude E Shannon. 1948. A mathematical theory of communication. *The Bell system technical journal*, 27(3):379–423.

Noam Shazeer. 2020. Glu variants improve transformer. *arXiv preprint arXiv:2002.05202*.

Noam Shazeer, Azalia Mirhoseini, Krzysztof Maziarz, Andy Davis, Quoc Le, Geoffrey Hinton, and Jeff Dean. 2017. Outrageously large neural networks: The sparsely-gated mixture-of-experts layer. *arXiv preprint arXiv:1701.06538*.

Anant Subramanian, Danish Pruthi, Harsh Jhamtani, Taylor Berg-Kirkpatrick, and Eduard Hovy. 2018. Spine: Sparse interpretable neural embeddings. In *Proceedings of the AAAI conference on artificial intelligence*, volume 32.

Christian Szegedy, Wojciech Zaremba, Ilya Sutskever, Joan Bruna, Dumitru Erhan, Ian Goodfellow, and Rob Fergus. 2013. Intriguing properties of neural networks. *arXiv preprint arXiv:1312.6199*.

Jihoon Tack, Jack Lanchantin, Jane Yu, Andrew Cohen, Ilia Kulikov, Janice Lan, Shibo Hao, Yuandong Tian, Jason Weston, and Xian Li. 2025. Llm pre-training with continuous concepts. *arXiv preprint arXiv:2502.08524*.

Glen Taggart. 2024. Prolu: A nonlinearity for sparse autoencoders - ai alignment forum.

Gemma Team, Morgane Riviere, Shreya Pathak, Pier Giuseppe Sessa, Cassidy Hardin, Surya Bhupatiraju, Léonard Hussenot, Thomas Mesnard, Bobak Shahriari, Alexandre Ramé, et al. 2024. Gemma 2: Improving open language models at a practical size. *arXiv preprint arXiv:2408.00118*.

Adly Templeton, Tom Conerly, Jonathan Marcus, Jack Lindsey, Trenton Bricken, Brian Chen, Adam Pearce, Craig Citro, Emmanuel Ameisen, Andy Jones, Hoagy Cunningham, Nicholas L Turner, Callum McDougall, Monte MacDiarmid, C. Daniel Freeman, Theodore R. Sumers, Edward Rees, Joshua Batson, Adam Jermyn, Shan Carter, Chris Olah, and Tom Henighan. 2024. Scaling monosemanticity: Extracting interpretable features from claude 3 sonnet. *Transformer Circuits Thread*.

Jesse Vig, Sebastian Gehrmann, Yonatan Belinkov, Sharon Qian, Daniel Nevo, Yaron Singer, and Stuart Shieber. 2020. Investigating gender bias in language models using causal mediation analysis. *Advances in neural information processing systems*, 33:12388–12401.

Benjamin Wright and Lee Sharkey. 2024. Addressing feature suppression in saes - ai alignment forum.

Xuansheng Wu, Wenhao Yu, Xiaoming Zhai, and Ninghao Liu. 2025a. Self-regularization with latent space explanations for controllable llm-based classification. *arXiv preprint arXiv:2502.14133*.

Xuansheng Wu, Jiayi Yuan, Wenlin Yao, Xiaoming Zhai, and Ninghao Liu. 2025b. Interpreting and steering llms with mutual information-based explanations on sparse autoencoders. *arXiv preprint arXiv:2502.15576*.

Zhengxuan Wu, Aryaman Arora, Atticus Geiger, Zheng Wang, Jing Huang, Dan Jurafsky, Christopher D. Manning, and Christopher Potts. 2025c. Axbench: Steering llms? even simple baselines outperform sparse autoencoders. *Preprint*, arXiv:2501.17148.

xAI. 2025. Grok 3 beta — the age of reasoning agents. Blog post announcing Grok 3 Beta, describing improvements in reasoning capabilities and performance benchmarks.

Xianjun Yang, Shaoliang Nie, Lijuan Liu, Suchin Gururangan, Ujjwal Karn, Rui Hou, Madian Khabsa, and Yuning Mao. 2025. Diversity-driven data selection for language model tuning through sparse autoencoder. *arXiv preprint arXiv:2502.14050*.

Qingyu Yin, Chak Tou Leong, Hongbo Zhang, Minjun Zhu, Hanqi Yan, Qiang Zhang, Yulan He, Wenjie Li, Jun Wang, Yue Zhang, et al. 2024. Direct preference optimization using sparse feature-level constraints. *arXiv preprint arXiv:2411.07618*.

Haiyan Zhao, Hanjie Chen, Fan Yang, Ninghao Liu, Huiqi Deng, Hengyi Cai, Shuaiqiang Wang, Dawei Yin, and Mengnan Du. 2024a. Explainability for large language models: A survey. *ACM Transactions on Intelligent Systems and Technology*, 15(2):1–38.

Haiyan Zhao, Fan Yang, Bo Shen, Himabindu Lakkaraju, and Mengnan Du. 2024b. Towards uncovering how large language model works: An explainability perspective. *arXiv preprint arXiv:2402.10688*.

Haiyan Zhao, Heng Zhao, Bo Shen, Ali Payani, Fan Yang, and Mengnan Du. 2025. Beyond single concept vector: Modeling concept subspace in llms with gaussian distribution. *The Thirteenth International Conference on Learning Representations*.

A Why Sparse Autoencoders?

As LLMs continue to grow rapidly in size, interpretation becomes more challenging, as the complexity of their latent space and internal representations also expands exponentially. SAEs have emerged as a powerful tool to understand how LLMs make decisions. This ability is known as mechanistic interpretability, which aims to reverse-engineer models by breaking down their internal computations into understandable, interpretable components. SAE is designed to learn a sparse, linear, and decomposable representation of the internal activations of a LLM. It enforces a sparsity constraint so that only a few features are active at any given time. This encourages each active feature to correspond to a specific, understandable concept. This simplification allows researchers to focus on a few key features rather than being overwhelmed by the full complexity of the model. Below, we discuss the development history of the SAE for LLMs and present Figure 1b to visually depict this progress. Due to page limitations, we do not attempt to provide an exhaustive history of SAEs, but instead focus on highlighting key milestones in the development of *SAEs for mainstream LLMs.*

Explaining Individual Neurons.
The development of interpretability techniques for LLMs has progressed in stages rather than as a single step. From 2022 to 2023, researchers at OpenAI and Anthropic focused on understanding LLMs by examining individual neurons. OpenAI, for instance, leveraged GPT-4 to generate natural language explanations for neurons in models like GPT-2, attempting to map specific neuron activations to concrete linguistic or conceptual features (Bills et al., 2023). Similarly, Anthropic built small toy models trained on synthetic data to observe how features are stored in neurons. These early investigations showed that analyzing single neurons can provide initial insights (Elhage et al., 2022). In addition, it is worth noting that the study of explaining individual neurons by labeling interpretable features to them has been extensively explored in studies (Radford et al., 2017; Donnelly and Roegiest, 2019; Nguyen et al., 2019; Szegedy et al., 2013) prior to the introduction of mechanistic interpretability.

However, they soon discovered that analyzing individual neurons had significant limitations, as neurons in LLMs often exhibit *polysemanticity*, i.e., responding to multiple unrelated inputs within the same neuron. For instance, a single neuron might simultaneously activate for academic citations, English dialogue, HTTP requests, and Korean text (Bricken et al., 2023). This phenomenon is largely attributed to *superposition*, where neural networks represent more independent features than available neurons by encoding each feature as a linear combination of neurons (Ferrando et al., 2024). While this architectural efficiency allows models to encode vast amounts of knowledge, it makes individual neurons difficult to interpret since their activations represent entangled mixtures of different concepts. This fundamental challenge with neuron-level analysis motivated researchers to explore more sophisticated approaches for disentangling these superimposed features, leading to the development of sparse autoencoders (SAEs) as a promising solution for extracting interpretable, monosemantic features from the model's complex internal representations.

SAEs for Small-size Language Models.
In late 2023, Anthropic advanced transformer interpretability by moving beyond raw neuron activations to decompose model activations into single-concept, monosemantic features, addressing the polysemanticity of individual neurons in LLMs (Cunningham et al., 2023; Bricken et al., 2023). They trained SAEs on transformer activation data by optimizing a reconstruction loss with a strong sparsity constraint. This training forces the autoencoder to represent each activation as a sparse combination of basis vectors, with each basis vector ideally capturing a distinct, interpretable concept. SAEs transform the overlapping signals of individual neurons into a set of clean, monosemantic features that are much easier to understand. This approach offers a clear advantage over traditional neuron-based methods by isolating the key features that drive model behavior. The promising experimental results on simpler transformer models demonstrated that SAEs provide a more effective and scalable route for interpreting model internals. Building on this success, later works Bloom (2024) and Samuel et al. (2024) applied SAE techniques to smaller models such as GPT-2 (Radford et al., 2019) and Pythia-70m (Biderman et al., 2023), thereby paving the way for their eventual extension to full-scale billion size LLMs.

SAEs for Large Language Models.
After witnessing the success of SAEs on smaller-scale models, the third stage of their development

emerged in 2024, when Anthropic (Templeton et al., 2024) and OpenAI (Gao et al., 2025) became the first groups to apply SAEs to their latest proprietary LLMs, Claude 3 Sonnet and GPT-4, respectively. This marked a significant step forward in understanding these closed-source, black-box models, even for the researchers who built them. However, scaling SAEs from small models to full-scale LLMs introduced several new challenges. One major issue was the sheer scale of activations in models with billions of parameters, which made training and extracting interpretable features computationally expensive. Additionally, ensuring that extracted features remained monosemantic became increasingly difficult, as feature superposition is more prevalent in larger models (Templeton et al., 2024). Despite these challenges, researchers found that SAEs could effectively decompose polysemantic neurons into monosemantic features, revealing meaningful and interpretable latent representations within the models. For instance, Anthropic demonstrated that certain neurons in Claude 3 Sonnet encode high-level concepts such as "sycophantic praise", where phrases like "a generous and gracious man" strongly activate this feature. Similarly, OpenAI's research on GPT-4 identified a "humans have flaws" feature, which activates on phrases like "My Dad wasn't perfect (are any of us?) but he loved us dearly." These findings not only deepen our understanding of model behavior but also provide powerful interpretability tools, allowing the practitioners to better analyze, refine, and steer language model outputs.

As the architecture and mechanisms of SAEs become clearer, more researchers have begun to follow this approach, applying SAEs to interpret open-source models. For example, Google Deep-Mind (Lieberum et al., 2024) used SAEs to analyze Gemma 2 (Team et al., 2024), while He et al. (2024) applied similar techniques to LLaMA 3.1 (Dubey et al., 2024). This growing adoption highlights the increasing role of SAEs in mechanistic interpretability, paving the way for broader transparency in both close- and open-source LLMs.

B Connection of SAEs to the Broader Field of Interpretability

The field of mechanistic interpretability (MI) has been critiqued for its insufficient engagement with the broader interpretability and NLP research literature (Bereska and Gavves, 2024a; Saphra and Wiegreffe, 2024). Many of the research topics within MI, such as polysemanticity, superposition, and SAEs, have been investigated in prior and concurrent non-MI fields, often under different terminologies while addressing the same fundamental challenges (Saphra and Wiegreffe, 2024; Elhage et al., 2022). For instance, the study of polysemanticity and superposition, which aims to understand how features are encoded in the model activations, have been studied in the context of distributed representations (Hinton, 1984; Mikolov et al., 2013b,a; Arora et al., 2018; Olah, 2023), disentangled representations (Higgins et al., 2018; Kim and Mnih, 2018; Locatello et al., 2019), and concept-based interpretability (Nicolson et al., 2024; Kim et al., 2018). Similarly, SAEs are closely related to and draw inspiration from earlier lines of research on sparse coding and dictionary learning (Olshausen and Field, 1997; Gregor and LeCun, 2010; Faruqui et al., 2015; Subramanian et al., 2018). These methods, like SAEs, posit the feature sparsity hypothesis (Elhage et al., 2022) and aim to learn an overcomplete representation to disentangle the features from activation in superposition. Since these fields pursue similar goals or study the same research problems, the current disconnect causes issues such as missing relevant literature, hindering collaboration, unintentionally redefining established concepts, rediscovering existing techniques, and overlooking well-known baselines. Therefore, it is imperative for the MI community to bridge these gaps and more actively integrate findings from related non-MI research.

C Different SAE Variants

C.1 Improve Architecture

Gated SAE. The Gated SAE (Rajamanoharan et al., 2024a) is a modification of the standard SAE that aims to improve the trade-off between reconstruction fidelity and sparsity enforcement. Traditional SAEs suffer from shrinkage bias (Wright and Sharkey, 2024), where the L_1-norm regularization systematically underestimates feature activations, leading to reduced reconstruction accuracy. Inspired by Gated Linear Units (Dauphin et al., 2017; Shazeer, 2020), Gated SAEs replace the standard ReLU encoder with a gated ReLU encoder, which separates the roles of detecting which features are active and estimating their magnitudes. Compared to traditional SAEs, this architectural separation addresses the shrinkage effect caused by L1 regular-

ization, which adds a linear penalty to all nonzero activations, leading to systematic underestimation of feature magnitudes.

$$\tilde{h}(\mathbf{z}) = \mathbf{1}\left[\pi_{\text{gate}}(\mathbf{z}) > 0\right] \odot \text{ReLU}(\pi_{\text{mag}}(\mathbf{z})), \quad (9)$$

where $\pi_{\text{gate}}(\mathbf{z}) = \mathbf{W}_{\text{gate}}(\mathbf{z} - \mathbf{b}_{\text{dec}}) + \mathbf{b}_{\text{gate}}$ is the gating function that determines which features should be activated. $\mathbf{W}_{\text{gate}}$ is a weight matrix for feature selection. $\pi_{\text{mag}}(\mathbf{z}) = \mathbf{W}_{\text{mag}}(\mathbf{z} - \mathbf{b}_{\text{dec}}) + \mathbf{b}_{\text{mag}}$ is the magnitude estimation function that determines the strength of the active features. $\mathbf{W}_{\text{mag}}$ is a weight matrix for magnitude estimation. $\mathbf{1}[\cdot]$ is the Heaviside step function that binarizes activations and $\odot$ denotes element-wise multiplication. In this case, Gated SAEs introduce independent pathways for determining which features are activated and their respective strengths, reducing bias and improving interpretability.

To optimize the Gated SAE, the authors introduce an auxiliary loss $\|\mathbf{z} - \hat{\mathbf{z}}_{\text{frozen}}\left(\text{ReLU}\left(\pi_{\text{gate}}(\mathbf{z})\right)\right)\|_2^2$ on top of the traditional loss function. This encourages the gating path to produce useful feature selections for reconstruction, without affecting the learned decoder weights. Here, $\hat{\mathbf{z}}_{\text{frozen}}$ is a copy of the decoder with frozen weights.

TopK SAE. The TopK SAE (Gao et al., 2025) is an improvement over the traditional SAE, designed to directly enforce sparsity without requiring L_1-norm regularization. Instead of penalizing all activations, which can introduce shrinkage bias, TopK SAEs enforce sparsity by retaining only the top K largest activations and setting the rest to zero. This ensures that only the most important features contribute to the learned representation. The encoder applies a linear transformation followed by a hard TopK selection:

$$\tilde{h}(\mathbf{z}) = \text{TopK}\left(\mathbf{W}_{\text{enc}}(\mathbf{z} - \mathbf{b}_{\text{pre}})\right), \quad (10)$$

where $\mathbf{W}_{\text{enc}} \in \mathbb{R}^{d \times m}$ is the encoder weight matrix, and $\mathbf{b}_{\text{pre}} \in \mathbb{R}^m$ is a pre-normalization bias term applied before the TopK selection.

Since the sparsity constraint is explicitly enforced through the TopK operation, there is no need for an additional sparsity regularization term in the loss function. The training objective reduces to minimizing the reconstruction loss:

$$\mathcal{L}(\mathbf{z}) = \|\mathbf{z} - \hat{\mathbf{z}}\|_2^2 + \alpha \mathcal{L}_{\text{aux}}, \quad (11)$$

where $\mathcal{L}_{\text{aux}}$ is an auxiliary loss scaled by the coefficient α, designed to stabilize training and prevent dead latents (Templeton et al., 2024).

BatchTopK SAE. The BatchTopK SAE is a modification of the TopK SAE, designed to address the limitations of enforcing a fixed number of active features per sample. Bussmann et al. (2024) identified two key inefficiencies in the standard TopK SAE. First, it forces every token to use exactly K features, even when some tokens may require fewer or more active features. It also does not allow flexibility across a batch, leading to inefficient sparsity control. To overcome these issues, BatchTopK SAEs apply the TopK selection globally across the entire batch instead of enforcing it per token. This means that BatchTopK selects the top $K \times B$ activations across the entire batch, where B is the batch size. The encoder is modified to:

$$\tilde{h}(\mathbf{Z}) = \text{BatchTopK}\left(\mathbf{W}_{\text{enc}}(\mathbf{Z} - \mathbf{b}_{\text{pre}})\right), \quad (12)$$

where $\mathbf{Z} \in \mathbb{R}^{B \times d}$ is the input batch matrix, and B is the batch size. Similar to TopK SAE, Batch-TopK directly controls sparsity through the selection mechanism, it eliminates the need for explicit sparsity regularization: $\mathcal{L}(\mathbf{Z}) = \|\mathbf{Z} - \hat{\mathbf{Z}}\|_2^2 + \alpha \mathcal{L}_{\text{aux}}$.

ProLU SAE. The ProLU SAE (Taggart, 2024) introduces a novel activation function called Proportional ReLU, which serves as an alternative to ReLU in traditional SAEs. ProLU SAE provides a Pareto improvement over both standard SAEs with L_1-norm regularization, which suffer from shrinkage bias, and SAEs trained with a Sqrt(L_1) penalty, which attempt to mitigate shrinkage but still do not fully address inconsistencies in activation scaling. In contrast to ReLU, which applies a fixed threshold at zero, ProLU introduces a learnable threshold for each activation, allowing the model to determine the optimal activation boundary dynamically. The ProLU activation function is defined as:

$$\text{ProLU}(m_i, b_i) = \begin{cases} m_i, & \text{if } m_i + b_i > 0 \text{ and } m_i > 0 \\ 0, & \text{otherwise} \end{cases},$$

$$(13)$$

where m_i is the pre-activation output from the encoder, and b_i is a learnable bias term that shifts the activation threshold. The encoding process in ProLU SAE replaces the standard ReLU activation with ProLU, leading to the following encoding function:

$$\tilde{h}(\mathbf{z}) = \text{ProLU}((\mathbf{z} - \mathbf{b}_{\text{dec}})\mathbf{W}_{\text{enc}}, \mathbf{b}_{\text{enc}}). \quad (14)$$

The ProLU SAE training objective consists of the standard reconstruction loss combined with an auxiliary sparsity term:

$$\mathcal{L}(\mathbf{z}) = \|\mathbf{z} - \hat{\mathbf{z}}\|_2^2 + \lambda P(\tilde{h}(\mathbf{z})), \quad (15)$$

where λ is the sparsity penalty coefficient, and $P(\tilde{h}(\mathbf{z}))$ is a sparsity-inducing function. The authors found that using a Sqrt(L_1) penalty, defined as $P(h) = \|h\|_{1/2}$, provided better sparsity control compared to the standard L_1-norm.

JumpReLU SAE. The JumpReLU SAE (Rajamanoharan et al., 2024b) is a modification of the traditional SAE that replaces the standard ReLU activation function with JumpReLU. The ReLU activation function sets all negative pre-activation values to zero but allows small positive values, leading to false positives in feature selection and underestimation of feature magnitudes. JumpReLU introduces an explicit threshold θ that zeroes out pre-activations below this threshold, ensuring that weak activations do not contribute to the reconstruction. The JumpReLU activation function is defined as:

$$\text{JumpReLU}_\theta(\mathbf{z}) = \mathbf{z} \cdot H(\mathbf{z} - \theta), \quad (16)$$

where θ is a learnable threshold and $H(x)$ is the Heaviside step function, which is 1 when $x > 0$ and 0 otherwise. The encoder in JumpReLU SAE follows a standard linear transformation followed by JumpReLU activation:

$$\tilde{h}(\mathbf{z}) = \text{JumpReLU}_\theta(\mathbf{W}_{\text{enc}}\mathbf{z} + \mathbf{b}_{\text{enc}}). \quad (17)$$

Unlike traditional SAEs that use L_1-norm for sparsity regularization, JumpReLU SAEs directly optimize the L_0-norm, which counts the number of nonzero activations: $\mathcal{L}(\mathbf{z}) = \|\mathbf{z} - \hat{\mathbf{z}}\|_2^2 + \alpha\|h(\mathbf{z})\|_0$.

Switch SAE. Inspired by Mixture of Experts (MoE) models (Shazeer et al., 2017), Switch SAE (Mudide et al., 2024) introduces a more computationally efficient framework for training SAEs. Instead of training a single large SAE, Switch SAE leverages multiple smaller "expert SAEs" $E_1, E_2, ..., E_N$ and a routing network that dynamically assigns each input to an appropriate expert. This approach enables efficient scaling to a large number of features while avoiding the memory and FLOP bottlenecks of traditional SAEs. Each "expert SAE" follows a standard TopK SAE formulation:

$$E_i(\mathbf{z}) = \mathbf{W}_{\text{dec}}^{(i)} \cdot \text{TopK}(\mathbf{W}_{\text{enc}}^{(i)}\mathbf{z}), \quad (18)$$

where $\mathbf{W}_{\text{enc}}^{(i)}$ and $\mathbf{W}_{\text{dec}}^{(i)}$ are the encoder and decoder weight matrices for expert i. The routing network determines which expert is assigned to each input

by computing a probability distribution over the experts:

$$p(\mathbf{z}) = \text{softmax}(\mathbf{W}_{\text{router}}(\mathbf{z} - \mathbf{b}_{\text{router}})), \quad (19)$$

where $\mathbf{W}_{\text{router}}$ is the routing weight matrix. $\mathbf{b}_{\text{router}}$ is the bias term. $p(\mathbf{z})$ represents the probability of selecting each expert. The final reconstruction is computed as:

$$\hat{\mathbf{z}} = p_{i^*(\mathbf{z})}E_{i^*(\mathbf{z})}(\mathbf{z} - \mathbf{b}_{\text{pre}}) + \mathbf{b}_{\text{pre}}, \quad (20)$$

where $i^*(\mathbf{z})$ is the selected expert for input $\mathbf{z}$.

To ensure balanced expert utilization and avoid expert collapse, Switch SAE incorporates an auxiliary loss for load balancing:

$$\mathcal{L}_{\text{aux}} = N \sum_{i=1}^{N} f_i \cdot P_i, \quad (21)$$

where f_i is the fraction of activations assigned to expert i, and P_i is the fraction of router probability assigned to expert i. This auxiliary loss is then added to the traditional reconstruction loss function to form the final learning objective.

C.2 Improve Training Strategy

Layer Group SAE. Traditionally, one SAE is trained per layer in a transformer-based LLM, resulting in a substantial number of parameters and high computational costs. To address this inefficiency, the Layer Group SAE (Ghilardi et al., 2024) clusters multiple layers into groups based on activation similarity and trains a single SAE per group. This significantly reduces training time while preserving reconstruction accuracy and interpretability. To determine which layers should be grouped together, the method measures the angular similarity between layer activations, defined as:

$$d_{\text{angular}}(\mathbf{z}_{\text{post}}^p, \mathbf{z}_{\text{post}}^q) = \frac{1}{\pi} \arccos\left(\frac{\mathbf{z}_{\text{post}}^p \cdot \mathbf{z}_{\text{post}}^q}{\|\mathbf{z}_{\text{post}}^p\|_2 \|\mathbf{z}_{\text{post}}^q\|_2}\right),$$
$$(22)$$

where $\mathbf{z}_{\text{post}}^p$ and $\mathbf{z}_{\text{post}}^q$ represent post-MLP residual stream activations for layers p and q. Using this similarity metric, layers with highly correlated activations are clustered together through a hierarchical clustering strategy. The number of groups K is chosen based on a computational trade-off, balancing efficiency and reconstruction accuracy. Once the layer groups are formed, a single SAE is trained per group instead of one per layer. The SAE architecture and training objective remains

similar as in traditional SAEs, optimizing for both reconstruction accuracy and sparsity.

Feature Choice SAE. Traditional SAEs face several limitations, including dead features, fixed sparsity per token, and lack of adaptive computation. Feature Choice SAEs (Ayonrinde, 2024) address these issues by imposing a constraint on the number of tokens each feature can be active for, rather than restricting the number of active features per token. This approach ensures that all features are utilized efficiently, preventing feature collapse and improving reconstruction accuracy. This sparsity allocation constraint is defined as:

$$\sum_j S_{i,j} = m, \forall i, \text{ where } M = mF, \quad (23)$$

where $S_{i,j}$ is a binary selection matrix, indicating whether feature i is active for token j. Each feature must be activated for exactly m tokens, enforcing uniform feature utilization.

Mutual Choice SAE. Mutual Choice SAE (Ayonrinde, 2024) remove all constraints on sparsity allocation, allowing the model to freely distribute its limited total sparsity budget across all tokens and features. Unlike TopK SAEs, which enforce a fixed number of active features per token, or Feature Choice SAEs, which constrain the number of tokens each feature can be assigned to, Mutual Choice SAE introduce global sparsity allocation. This means that instead of enforcing a per-token or per-feature selection, the model selects the top M feature-token matches across the entire dataset, ensuring that sparsity is allocated adaptively based on reconstruction needs. Mathematically, the activation selection process is defined as:

$$S = \text{TopKIndices}(\mathbf{Z}', M), \quad (24)$$

where $\mathbf{Z}'$ represents the pre-activation affinity matrix between tokens and features. M is the global sparsity budget, denoting the total number of active feature-token pairs allowed. $\text{TopKIndices}(\cdot)$ selects the top M activations globally, instead of enforcing a fixed K per token.

Feature Aligned SAE. The Feature Aligned SAE (Marks et al., 2024) introduces Mutual Feature Regularization (MFR), a novel training method designed to improve the interpretability and fidelity of learned features in SAEs. Traditional SAEs often suffer from feature fragmentation, where meaningful input features get split across multiple decoder weights, and feature entanglement, where multiple independent input features are merged into a single decoder weight. These issues reduce the interpretability of SAEs and limit their effectiveness in analyzing neural activations. The key insight behind MFR is that features learned by multiple SAEs trained on the same dataset are more likely to align with the true underlying structure of the input data. To enforce this, Feature Aligned SAE trains multiple SAEs in parallel and applies a MFR penalty that encourages them to learn mutually consistent features:

$$\mathcal{L}_{\text{MFR}} = \alpha \left(\frac{1}{N(N-1)} \sum_{i=1}^{N-1} \sum_{j=i+1}^{N} (1 - \text{MMCS}(\mathbf{W}_{dec}^{(i)}, \mathbf{W}_{dec}^{(j)})) \right), \quad (25)$$

where $\mathbf{W}_{dec}^{(i)}$ and $\mathbf{W}_{dec}^{(j)}$ are the decoder weight matrices of different SAEs. Mean of Max Cosine Similarity (MMCS) measures the degree of alignment between the learned features across SAEs. α is a hyperparameter that controls the strength of the regularization. This mutual feature regularization is then combined with the traditional SAE loss to form the final training objective of the Feature Aligned SAE.

End-to-end SAE. Traditional SAEs often prioritize minimizing reconstruction error rather than ensuring that learned features are functionally important to the model's decision-making. This often leads to feature splitting, where a single meaningful feature is divided into multiple redundant components. To address this, End-to-end SAE (Braun et al., 2025) modifies the training objective to ensure that the discovered features directly influence the network's output. They propose minimizing the Kullback-Leibler (KL) divergence between the original network's output distribution and the output distribution when using SAE activations, formulated as:

$$\mathcal{L}_{\text{e2e}} = KL(\hat{y}, y) + \alpha \|h(\mathbf{z})\|_1. \quad (26)$$

To further ensure that activations follow similar computational pathways in later layers, they propose E2e + Downstream SAE, which introduces an additional downstream reconstruction loss, leading to the formulation:

$$\mathcal{L}_{\text{e2e+ds}} = KL(\hat{y}, y) + \alpha \|h(\mathbf{z})\|_1 + \beta \sum_{k=l+1}^{L} \|\hat{\mathbf{a}}^{(k)} - \mathbf{a}^{(k)}\|_2^2. \quad (27)$$

By shifting the training focus from activation reconstruction to output distribution preservation, this method ensures that learned features are more

aligned with the actual computational processes of the network while maintaining interpretability.

Formal Languages SAE. Traditional SAEs effectiveness remains questionable in language models due to their reliance on correlations rather than causal attributions. While SAEs often recover features that correlate with linguistic structures, such as parts of speech or syntactic depth, interventions on these features frequently do not influence the model's predictions, suggesting that current training objectives fail to ensure causal relevance. To address this, Formal Languages SAE (Menon et al., 2024) introduce a causal loss term that explicitly encourages SAEs to learn features that impact the model's computation. Their proposed loss function is given by:

$$L = L_{\text{recon}} + \alpha L_{\text{sparse}} + \beta L_{\text{caus}}, \qquad (28)$$

where L_{recon} is the standard reconstruction loss, L_{sparse} enforces sparsity, and L_{caus} ensures that interventions on learned features result in predictable changes in model output.

Specialized SAE. Traditional SAEs struggle to capture rare and low-frequency concepts, which are critical for understanding model behavior in specific subdomains. To address this, Specialized SAE (SSAE) (Muhamed et al., 2024) focuses on learning rare subdomain-specific features through targeted data selection and a novel training objective. Instead of training on the full dataset, SSAE uses high-recall dense retrieval methods, such as BM25, Contriever, and TracIn reranking, to identify relevant subdomain data, ensuring that rare features are well-represented. Additionally, they introduce Tilted Empirical Risk Minimization (TERM), an objective that optimizes for worst-case reconstruction loss rather than average loss. This is achieved by modifying the standard SAE loss function to:

$$L_{\text{TERM}}(t; w) = \frac{1}{t} \log \left(\frac{1}{N} \sum_{i=1}^{N} e^{t \cdot L_w(\mathbf{z_i})} \right), \quad (29)$$

where $L_w(\mathbf{z_i})$ is the standard SAE loss for representation $\mathbf{z_i}$. N is the size of a minibatch, and t is the tilt parameter that controls emphasis on rare concept reconstruction.

C.3 SAE Training

Even though the framework of SAEs is conceptually straightforward, training SAEs is both computationally expensive and data-intensive. The complexity arises due to the overcomplete dictionary representation, large-scale data requirements, and the layer-wise training paradigm necessary for interpreting LLMs. Each of these factors contributes to the substantial computational cost associated with training SAEs at scale.

Overcomplete Dictionary Representation. A defining characteristic of SAEs is their overcomplete dictionary, where the number of learned features far exceeds the dimensionality of the LLM's latent space. This overcompleteness is what enables SAEs to enforce sparsity, allowing them to isolate and extract meaningful feature activations from high-dimensional representations. The enforced sparsity is crucial for LLM interpretability, as it helps decompose complex neural activations into more semantically meaningful features. Empirical studies highlight the scale of overcompleteness; for example, LLaMa-Scope (He et al., 2024) trained SAEs with 32K and 128K features, which are 8× and 32× larger than the hidden size of LLaMa3.1-8B. This extreme overparameterization provides a highly expressive feature space but significantly increases the computational burden during training.

Large-Scale Data Requirements. Since the input to an SAE consists of representations from LLMs, an enormous amount of data is required to ensure that the model learns a diverse and representative set of activations. To effectively train an SAE, it is essential to activate a wide range of neurons in the LLM, which necessitates processing large-scale datasets covering diverse linguistic structures. Moreover, because SAEs are overcomplete, they require significantly more training data to converge. Empirical results from Gemma-Scope (Lieberum et al., 2024) illustrate this requirement: SAEs with 16.4K features were trained on 4 billion tokens, while 1M-feature SAEs required 16 billion tokens to reach satisfactory performance. This highlights the immense data demands necessary for training effective SAEs. Another challenge arises when scaling up the training data, which is how to efficiently shuffling massive datasets across distributed systems. Shuffling is crucial to prevent models from learning spurious, order-dependent patterns. However, as datasets grow to terabyte or petabyte scales, performing a distributed shuffle becomes a significant engineering hurdle (Anthropic, 2024).

Layer-Wise Training. Interpreting an LLM requires understanding its representations at each layer, which necessitates training separate SAEs

for different layers of the model. The standard approach is to train one SAE per layer, meaning that for deep models, this process must be repeated across dozens or even hundreds of layers, compounding the computational cost. The necessity of layer-wise training is further evidenced by ongoing research efforts attempting to reduce the number of SAEs required. For example, Layer Group SAE (Ghilardi et al., 2024), which we discussed previously, clusters multiple layers into layer groups and trains a single SAE per group instead of per layer. The emergence of such strategies demonstrates the significant computational burden imposed by layer-wise SAE training and the ongoing efforts to optimize it.

D Evaluation and Comparison of SAEs

As shown in Table 2, we evaluate three series of SAEs: LLaMa Scope, Pythia SAE, and Gemma Scope. For LLaMa Scope, we use the llama-scope-lxa-8x SAE trained on layer 12 of the LLaMa 3.1 8B model. For Pythia, we evaluate the sae-bench-pythia70m-sweep-standard-ctx128-0712 SAE, trained on layer 5 of the Pythia 70M model. Within the Gemma Scope, we conduct an internal comparison across five gemma-scope-2b-pt-res SAEs, all trained on layer 12 of the Gemma2 2B model. These five SAEs differ only in their training L0 sparsity settings, meaning they were trained to activate different numbers of latents per input.

We report both structural and functional evaluation metrics. The structural metrics, listed at the top, include L0 Sparsity, Mean Squared Error (MSE), Cross-Entropy Loss, KL Divergence, and Explained Variance. The functional metrics, shown below, including Absorption, Spurious Correlation Removal (SCR), and Sparse Probing. In the Absorption metric, mean absorption captures the fraction of cases where the correct SAE latents fail to activate for a known feature, while another latent with similar semantics activates instead. Full absorption refers to the stricter case where none of the correct latents activate and the feature is entirely absorbed by an unintended latent. In SCR, we assess how well the SAE reduces unwanted correlations. The Top-5, Top-50, and Top-500 SCR scores measure how much debiasing can be achieved by removing top 5, 50, 500 latents respectively. Finally, Sparse Probing evaluates whether the SAE has learned interpretable and disentangled concepts.

We compare the performance of sparse probes using SAE activations against a baseline probe using the LLM's original dense activations. Higher score indicates that the SAE has successfully learned concept-specific features.

Shown in Table 2, the LLaMa Scope SAE shows significantly higher L0 sparsity (869.3) compared to the others. The Gemma Scope SAEs span a range of sparsities, from highly sparse (L0:22 with 22.1 active latents) to relatively dense (L0:445 with 472.2). Within the Gemma Scope series, we observe that as sparsity denser, the MSE also decreases, indicating improved reconstruction accuracy. Similarly, both the cross-entropy loss and KL divergence scores increase toward 1, suggesting that denser SAEs preserve the model's original predictive behavior more. The explained variance also improves with denser sparsity, rising from 0.824 at L0:22 to 0.941 at L0:445, which shows that denser SAEs are better at capturing the variance of the original activations.

In functional metrics, LLaMa Scope exhibits extremely low mean and full absorption values (0.0028 and 0.00047), likely due to its high redundancy from overactivation. Among the Gemma Scope models, L0:176 achieves the lowest mean (0.055) and full (0.038) absorption, suggesting a good trade-off between sparsity and disentanglement. Later, absorption increases again at L0:445, indicating that overly dense SAEs may begin to recombine multiple concepts into the same latent. Looking at SCR, all SAEs' performance improves with top-k increase. However, SCR scores begin to decrease at Top-500, indicating that over-ablation may unintentionally remove useful features. For Sparse Probing, we can see that across all models, SAE probes perform nearly as well as LLM-based probes, with accuracies consistently above 0.95 for Gemma Scope. Notably, the Pythia SAE and Gemma Scope L0:445 achieve sparse probing accuracies that even exceed the LLM baseline, suggesting that these models successfully capture clean, task-relevant features using a small set of latents.

E Other Applications of SAEs in LLMs

E.1 Model Training

SAEs are trained to obtain more sparse and interpretable features. The learned concepts and sparsity are both beneficial in model transparency, which can be utilized in model training to align the model with human understanding and improve

Table 2: Evaluation of SAEs

		LLaMa Scope	Pythia SAE	Gemma Scope				
				L0:22	L0:41	L0:82	L0:176	L0:445
Structural	Sparsity	869.318	112.888	22.141	41.422	80.472	174.74	472.199
	MSE	4.9E-5	0.015	2.125	1.836	1.539	1.203	0.707
	CE Loss	1.00	0.940	0.974	0.984	0.988	0.993	0.998
	KL Div	0.898	-1	0.975	0.984	0.990	0.994	0.997
	Variance	0.863	0.918	0.824	0.848	0.875	0.902	0.941
Absorption	Mean	2.8E-3	0.227	0.287	0.267	0.105	0.055	0.1347
	Full	4.7E-4	0.199	0.333	0.275	0.091	0.038	0.045
SCR	Top 5	0.137	0.330	0.206	0.217	0.210	0.184	0.243
	Top 50	0.713	0.414	0.376	0.385	0.407	0.417	0.384
	Top 500	-0.727	0.232	0.316	0.309	0.359	0.339	0.384
Sparse Probing	LLM	0.904	0.922			0.958		
	SAE	0.885	0.929	0.952	0.955	0.955	0.957	0.958

model performance. Since SAEs include feature-level constraints, Yin et al. (2024) leverage these constraints to enable sparsity-enforced alignment in post-training. Their experiments demonstrate that this approach achieves superior performance across benchmark datasets with reduced computational costs. Similarly, combine learned concepts with next-token prediction training to build more transparent models. Specifically, they extract influential concepts on outputs from SAEs, then incorporate these concept vectors into hidden states by modifying token embeddings. Results show that models trained with this method perform better and exhibit greater robustness on token prediction and knowledge distillation across benchmark datasets (Tack et al., 2025). Moreover, SAEs' ability to provide large-scale explanations has been well explored. By examining the diversity of activated features, Yang et al. (2025) developed a new approach to augment data diversity. Another work uses task-specific features learned in SAEs to mitigate unintended features within models, significantly improving model generalization on real-world tasks (Wu et al., 2025a).

F SAE and Probing-Based Methods

In addition to SAEs, probing-based methods have emerged as a prominent family of techniques for interpreting and steering the internal representations of LLMs (Giulianelli et al., 2018; Vig et al., 2020; Meng et al., 2022; Guerner et al., 2023; Geiger et al., 2023). These methods operate under the assumption that meaningful concepts are linearly separable within the model's representation space (Mikolov et al., 2013b; Pennington et al., 2014; Park et al., 2023; Nanda et al., 2023). Probing formulates steering as a supervised learning problem, which given a small set of labeled examples, the method learns low-rank projection vectors that can both detect and influence the presence of target concepts during generation.

Based on the recent research, SAEs show certain limitations compared to linear probes for language model interpretation. First, the AXBENCH study (Wu et al., 2025c) demonstrates that even simple linear probe baselines like difference-in-means consistently outperform SAEs on concept detection tasks, with SAEs falling behind on both concept detection and model steering benchmarks. Second, Kantamneni et al.'s comprehensive evaluation (Kantamneni et al., 2025) across 113 probing datasets reveals that SAEs fail to provide consistent advantages in challenging regimes like data scarcity, class imbalance, label noise, and covariate shift. There remains a long way for the SAE research community to go in making sparse autoencoders more robust, generalizable, and useful in practical applications before they can reliably outperform simpler interpretability approaches.

G Research Challenges

In this section, we outline several critical research challenges with SAEs. Although SAEs have emerged as promising tools for providing large-scale, fine-grained interpretable explanations, these challenges could threaten the faithfulness, effectiveness, and efficiency of their applications.

G.1 Incomplete Concept Dictionary

SAEs are trained on large corpora of data encompassing various concepts. However, achieving comprehensive concept coverage remains challenging (Muhamed et al., 2024). Additionally, the learning process of SAEs functions as a black box where learned concepts cannot be predetermined. Consequently, controlling the completeness of input and output concepts is nearly impossible. Furthermore, explanations provided by SAEs may be incomplete or misleading due to the conceptual gaps. This limitation can result in unreliable interpretations when applying SAEs to complex reasoning tasks that require comprehensive knowledge representation.

G.2 Lack Theoretical Foundations

The development of SAEs is indeed based on assumptions of superposition and linear concept representation. Empirically, we've found it effective to construct high-level features through linear combinations of low-level features. However, our understanding of how these concepts are represented in hidden spaces and their spatial relationships remains limited. This limitation explains why we must derive combination parameters empirically rather than mathematically. The validity and advancement of SAEs may remain unclear until we can properly demonstrate the correctness of these fundamental assumptions about concept representation and superposition in neural networks.

G.3 Reconstruction Errors

SAEs are trained by minimizing the reconstruction errors between original and reconstructed activations. However, these errors persist and remain poorly understood. Recent research by (Gao et al., 2025) demonstrates that reconstruction errors can produce significant performance degradation comparable to using a model with only 10% of the pretraining compute. This finding raises substantial concerns about SAE accuracy as interpretability tools. Furthermore, the impact of these reconstruction errors on model generations has not been adequately measured. The field lacks output-centric metrics that could precisely quantify how reconstructed activations affect a model's final outputs. To advance our understanding of SAEs and their reliability as interpretability tools, developing metrics that directly measure the effect of reconstruction errors on generated content is essential.

G.4 Computational Burden

SAEs operate at the layer level for each model, mapping original activations to a much higher-dimensional representation space before reconstructing them back to the original space. This architecture necessitates that SAE parameters for a specific layer significantly outnumber the parameters of that original layer itself. Consequently, the overall training computation exceeds that of the original model training, particularly problematic for LLMs with billions of parameters. The extensive computational resources required create a substantial barrier for researchers interested in investigating these methods. Furthermore, SAEs exhibit limited transferability across models, they must be trained specifically for each model and each layer, exacerbating the computational burden. This layer-specific and model-specific training requirement multiplies the already significant resource demands, further restricting accessibility for the broader research community.